

EGF-mediated induction of Mcl-1 at the switch to lactation is essential for alveolar cell survival

Nai Yang Fu^{1,2}, Anne C. Rios^{1,2,10}, Bhupinder Pal^{1,2,10}, Rina Soetanto³, Aaron T. L. Lun^{2,4}, Kevin Liu^{1,2}, Tamara Beck^{1,2}, Sarah A. Best^{1,2}, François Vaillant^{1,2}, Philippe Bouillet^{2,5}, Andreas Strasser^{2,5}, Thomas Preiss^{3,6}, Gordon K. Smyth^{4,7}, Geoffrey J. Lindeman^{1,8,9,10} and Jane E. Visvader^{1,2,10,11}

Expansion and remodelling of the mammary epithelium requires a tight balance between cellular proliferation, differentiation and death. To explore cell survival versus cell death decisions in this organ, we deleted the pro-survival gene *Mcl-1* in the mammary epithelium. *Mcl-1* was found to be essential at multiple developmental stages including morphogenesis in puberty and alveologenesis in pregnancy. Moreover, *Mcl-1*-deficient basal cells were virtually devoid of repopulating activity, suggesting that this gene is required for stem cell function. Profound upregulation of the *Mcl-1* protein was evident in alveolar cells at the switch to lactation, and *Mcl-1* deficiency impaired lactation. Interestingly, EGF was identified as one of the most highly upregulated genes on lactogenesis and inhibition of EGF or mTOR signalling markedly impaired lactation, with concomitant decreases in *Mcl-1* and phosphorylated ribosomal protein S6. These data demonstrate that *Mcl-1* is essential for mammopoiesis and identify EGF as a critical trigger of *Mcl-1* translation to ensure survival of milk-producing alveolar cells.

Unlike most tissues, the mammary gland exists as a rudimentary tree at birth and predominantly develops in the postnatal animal¹. Morphogenesis during puberty is characterized by ductal elongation and branching to form an elaborate ductal tree, which comprises an inner layer of luminal cells and an outer layer of myoepithelial cells adjacent to the basement membrane. During pregnancy, the mammary epithelium undergoes massive expansion, with the formation of alveolar structures that terminally differentiate into secretory units in late pregnancy to enable lactation. Following weaning, these alveolar structures regress through programmed cell death, thus returning the gland to a virgin-like state. Two primary forms of cell death have been implicated in the involution process, apoptosis² and more recently, lysosomal-mediated death³ that occurs independently of caspases³. However, the molecular regulators that control cell death versus survival decisions in the mammary gland are poorly defined.

The Bcl-2 protein family members act as the arbiters of the intrinsic apoptotic pathway^{4,5} and comprise pro-survival members (for example, Bcl-2, Mcl-1, Bcl-X_L), initiators of apoptosis (for

example, Bim), and the downstream effector proteins Bak and Bax. Whether or not any member of the Bcl-2 family plays an essential role in the mammary gland remains an important question. Loss of *Bcl-x* (ref. 6) causes mild abnormalities in involution, whereas loss of *Bim*⁷ is associated with a transient phenotype in puberty, in which clearing of the luminal space of terminal endbuds and terminal ducts was delayed. In other tissues, the pro-survival protein *Mcl-1* has been shown to be critical for the survival of diverse cell types, including haematopoietic stem cells⁸, lymphocytes^{9,10}, neutrophils^{11,12}, neurons^{13,14} and cardiomyocytes^{15,16}. Here we have explored the role and regulation of *Mcl-1* in mammopoiesis.

RESULTS

Mcl-1 expression is markedly upregulated in luminal cells during lactation

Analysis of *Mcl-1* expression revealed that its protein levels varied substantially between the different mammary developmental stages. Profound upregulation of *Mcl-1* was evident at the onset of lactation, in contrast to the very low levels of *Mcl-1* present at

¹ACRF Stem Cells and Cancer Division, The Walter and Eliza Hall Institute of Medical Research, Parkville, Victoria 3052, Australia. ²Department of Medical Biology, The University of Melbourne, Parkville, Victoria 3010, Australia. ³Genome Biology Department, The John Curtin School of Medical Research, The Australian National University, Canberra, Australian Capital Territory 0200, Australia. ⁴Bioinformatics Division, The Walter and Eliza Hall Institute of Medical Research, Parkville, Victoria 3052, Australia. ⁵Molecular Genetics of Cancer Division, The Walter and Eliza Hall Institute of Medical Research, Parkville, Victoria 3052, Australia. ⁶Victor Chang Cardiac Research Institute, Darlinghurst, New South Wales 2010, Australia. ⁷Department of Mathematics and Statistics, The University of Melbourne, Parkville, Victoria 3010, Australia. ⁸Department of Medical Oncology, The Royal Melbourne Hospital, Parkville, Victoria 3050, Australia. ⁹Department of Medicine, The University of Melbourne, Parkville, Victoria 3010, Australia. ¹⁰These authors contributed equally to this work.

¹¹Correspondence should be addressed to J.E.V. (e-mail: visvader@wehi.edu.au)

Received 2 August 2014; accepted 19 January 2015; published online 2 March 2015; DOI: 10.1038/ncb3117

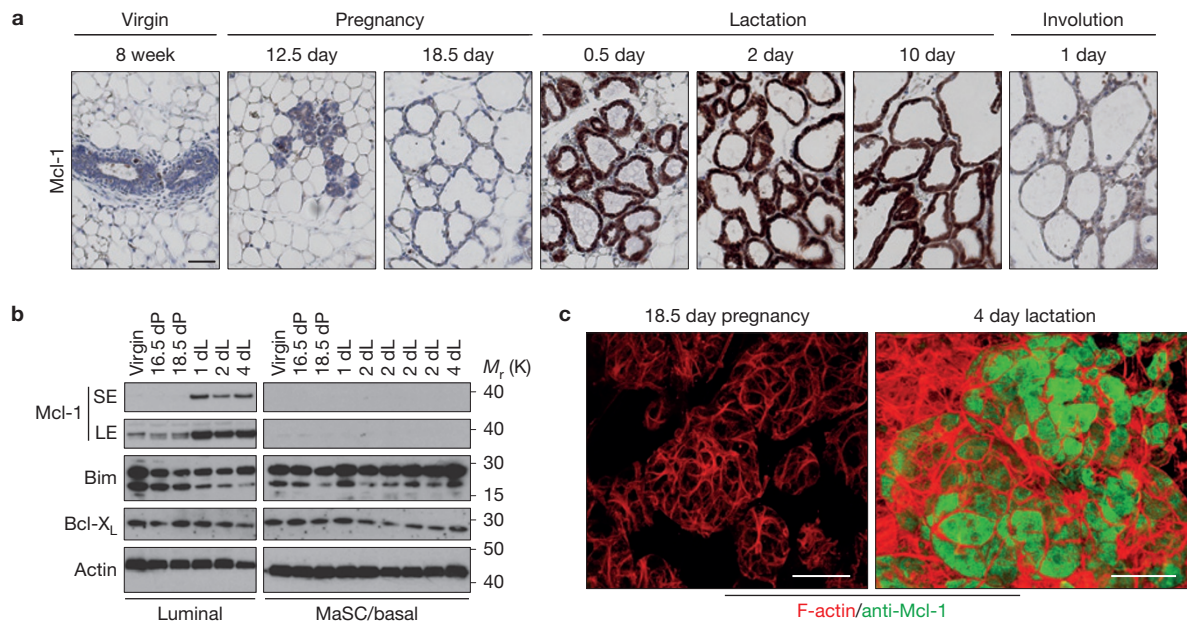


Figure 1 Dynamic expression of Mcl-1 protein levels during mammary gland development and involution. **(a)** Immunohistochemical staining for Mcl-1 expression in the mammary glands of FVB/N females at different development stages ($n=3$ mice per stage). Scale bar, 50 μ m. **(b)** Representative western blot analysis ($n=3$) of the expression of Bcl-2 family members in sorted luminal ($\text{Lin}^- \text{CD29}^{\text{lo}} \text{CD24}^+$) or MaSC/basal ($\text{Lin}^- \text{CD29}^{\text{hi}} \text{CD24}^+$) cells isolated from virgin, pregnant (16.5 and 18.5 days pregnant dP) or lactating (1, 2 and 4 days lactating dL) mammary glands of FVB/N mice. SE, short exposure; LE, long exposure. About 50,000 cells were used for each sample. **(c)** Three-dimensional whole-mount confocal analysis of Mcl-1 expression in the mammary glands of FVB/N mice at 18.5 days of pregnancy (18.5 dP) or 4 days of lactation (4 dL) (representative of $n=3$ experiments). Tissues were immunostained for Mcl-1. F-actin was stained by phalloidin to observe the entire tissue at the cellular level. Scale bars, 30 μ m (at 18.5 dP) and 50 μ m (at 4 dL). Uncropped images of blots are shown in Supplementary Fig. 7.

other stages of morphogenesis, based on both immunohistochemical and western blot analyses (Fig. 1a and Supplementary Fig. 1a). Evaluation of protein expression in freshly sorted cells (Supplementary Fig. 1b,c) from the mammary stem cell (MaSC)-enriched/basal (denoted MaSC/basal; CD29^{hi}CD24⁺) and luminal (CD29^{lo}CD24⁺) cell populations indicated that Mcl-1 upregulation was confined to alveolar luminal cells of the lactating gland and that expression was very low in the MaSC/basal subset across all of the development stages (Fig. 1b and Supplementary Fig. 1d,e). Confocal imaging in three dimensions¹⁷ verified that the Mcl-1 protein was induced exclusively in both ductal and alveolar luminal cells at the onset of lactation (Fig. 1c and Supplementary Fig. 2). In contrast to Mcl-1, Bcl-2 was markedly downregulated during pregnancy, whereas Bcl-XL levels remained unchanged through the different developmental stages (Fig. 1b and Supplementary Fig. 1d). Interestingly, Mcl-1 transcript levels were similar across development by quantitative PCR with reverse transcription (qRT-PCR), with an approximate twofold decrease in messenger RNA levels in luminal cells during lactation (Supplementary Fig. 1f). These data indicate that Mcl-1 expression is subject to post-transcriptional regulation at the onset of lactation. Indeed, there is substantial evidence for post-transcriptional and translational control of Mcl-1 expression in other systems^{18–20}.

Further fractionation of the luminal population into progenitor and mature subtypes²¹ showed that most Bcl-2 pro-survival proteins exhibited higher expression in the luminal progenitor (CD14⁺CD61⁺ and CD14⁺CD61⁻) relative to the mature luminal subset (CD14⁻CD61⁻) (Supplementary Fig. 1b,g). qRT-PCR analysis

exposure; LE, long exposure. About 50,000 cells were used for each sample. **(c)** Three-dimensional whole-mount confocal analysis of Mcl-1 expression in the mammary glands of FVB/N mice at 18.5 days of pregnancy (18.5 dP) or 4 days of lactation (4 dL) (representative of $n=3$ experiments). Tissues were immunostained for Mcl-1. F-actin was stained by phalloidin to observe the entire tissue at the cellular level. Scale bars, 30 μ m (at 18.5 dP) and 50 μ m (at 4 dL). Uncropped images of blots are shown in Supplementary Fig. 7.

Table 1 Limiting dilution analysis of the repopulating frequency of MaSC-enriched cells from Mcl-1-deficient and control mammary glands.

Genotype	Number of DP cells injected per fat pad	Number of outgrowths*	Repopulating frequency†
MMTV-cre/Mcl-1 ^{f/f}	50	0/6	Indeterminant
	100	0/6	
	200	0/6	
	400	0/6	
MMTV-cre/Mcl-1 ^{f/+}	50	4/5	1/86 (47–157)
	100	5/6	
	200	6/6	
	400	6/6	

Limiting dilution analysis of the repopulating frequency of MaSC/basal cells from MMTV-cre/Mcl-1^{f/f} mice. Freshly sorted Lin⁻CD29^{hi}CD24⁺hCD4⁺ (double positive, DP) cells from the mammary glands of 10-week-old MMTV-cre/Mcl-1^{f/f} or control littermate females were transplanted into the cleared fat pads of 3-week-old recipient mice. * shown as the number of outgrowths per number of injected fat pads. Only outgrowths that filled $\geq 10\%$ of the fat pad were scored. †Confidence interval 95%.

confirmed Mcl-1 expression in the different epithelial subpopulations, with lower levels evident in mature luminal cells (Supplementary Fig. 1h).

Loss of Mcl-1 impairs morphogenesis during puberty

To explore the physiological role of Mcl-1 in the mammary gland, we conditionally deleted Mcl-1 at different stages of mammapoiesis (Fig. 2a,b). We first used the human CD4 (hCD4) reporter gene incorporated into the Mcl-1 allele²² (Fig. 2a) to monitor Mcl-1 promoter activity at the single-cell level by flow cytometric analysis

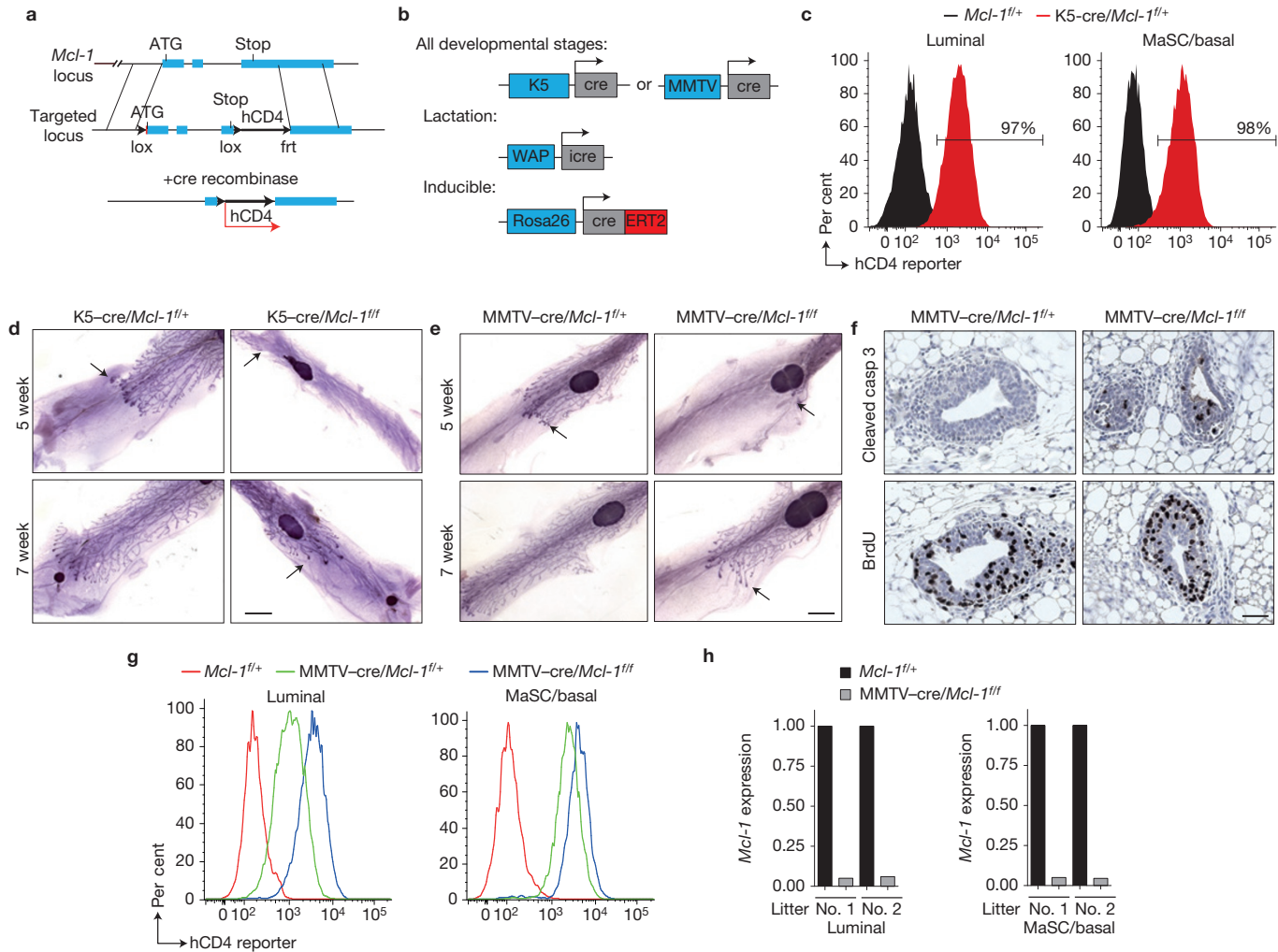


Figure 2 *Mcl-1* deletion impairs expansion of the mammary epithelium during puberty. (a) Schematic diagram of the floxed *Mcl-1* allele. The *Mcl-1* mutant allele contains two loxP sites and the coding sequence for a truncated form of human CD4 (hCD4). On cre-mediated recombination, the hCD4 reporter is expressed on the cell surface. (b) The different Cre strains used to delete *Mcl-1* in mammary epithelium. (c) Representative FACS plots demonstrating highly efficient recombination at the *Mcl-1* allele ($n=4$ independent experiments). More than 95% of both luminal and MaSC/basal cells from K5-cre/*Mcl-1*^{fl/fl} females expressed the hCD4 reporter but none could be detected in *Mcl-1*^{fl/fl} mammary epithelial cells. (d,e) Whole-mounted mammary glands from 5- or 7-week-old *Mcl-1*-deficient or littermate control mice from the K5-cre (d) or MMTV-cre (e) model ($n=3$ mice per

genotype). Scale bars, 2.5 mm. (f) Immunostaining of mammary glands from a representative 6-week-old MMTV-cre/*Mcl-1*^{fl/fl} female and a littermate control for cleaved caspase-3 and BrdU ($n=3$ independent experiments). Scale bar, 50 μ m. (g) Representative FACS plots ($n=4$) demonstrating highly efficient *Mcl-1* deletion from both floxed alleles in 10-week-old mice. Both luminal and MaSC/basal cells from MMTV-cre/*Mcl-1*^{fl/fl} females exhibit higher hCD4 reporter expression than littermate MMTV-cre/*Mcl-1*^{fl/fl} females ($n=6$ mice per genotype). (h) qRT-PCR analysis showing markedly reduced *Mcl-1* transcript levels in the luminal and MaSC/basal populations isolated from individual glands of 10-week-old MMTV-cre/*Mcl-1*^{fl/fl} mice compared with control mice (mean of 3 technical replicates for each point).

following cre-mediated recombination. CD4 reporter expression could be detected in more than 90% of cells in the MaSC/basal and luminal subsets isolated from K5-cre/*Mcl-1*^{fl/fl} glands (Fig. 2c). These results indicate active *Mcl-1* transcription in most mammary epithelial cells and efficient recombination at the *Mcl-1* locus by K5-cre.

Deletion of *Mcl-1* by either MMTV- or K5-cre was found to profoundly affect ductal morphogenesis during puberty. Only small mammary rudiments were present in 5-week-old MMTV-cre/*Mcl-1*^{fl/fl} or K5-cre/*Mcl-1*^{fl/fl} females and by 7 weeks, the ductal trees only half-filled the fat pad, in contrast to littermate control mice

(Fig. 2d,e). By 10–12 weeks of age, ductal elongation had largely been rescued, presumably owing to continual oestrus cycling. The mammary glands of heterozygous (MMTV-cre/*Mcl-1*^{fl/+} and K5-cre/*Mcl-1*^{fl/+}) (Fig. 2d,e) and cre-only mice were indistinguishable from wild-type mice. Immunostaining for cleaved (activated) caspase-3 revealed a marked difference on *Mcl-1* deletion: there were 0.9% versus 6.5% cleaved caspase-3-positive cells in the terminal endbuds of control and *Mcl-1*-deficient mammary glands at 6 weeks of age, respectively, with cells in >50 terminal endbuds scored (Fig. 2f; $n=4$ mice for each genotype; $P=0.005$, Student's *t*-test). No difference in the proportion of proliferating, BrdU-positive cells was

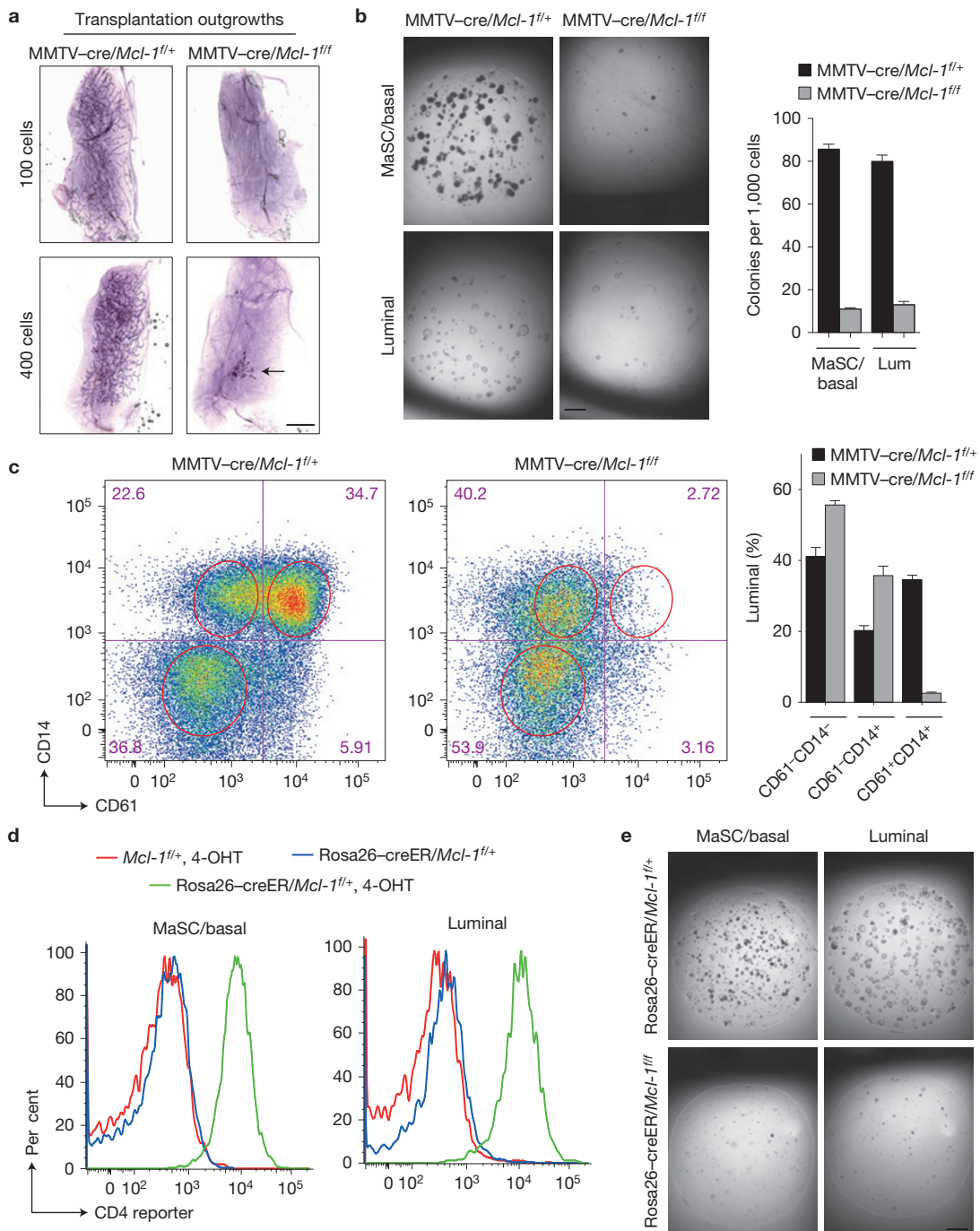


Figure 3 Mcl-1-dependent survival is essential for stem and progenitor cell activity. (a) Representative whole-mounts of outgrowths obtained after transplantation of 100 and 400 Lin-CD29^{hi}CD24⁺hCD4⁺ cells isolated from MMTV-cre/Mcl-1^{fl/fl} or control 10-week-old female mice. Less than 5% of the fat pad was filled in the case of MMTV-cre/Mcl-1^{fl/fl} cells (lower right panel). The arrow depicts the rudimentary outgrowth. See Table 1. Scale bar, 2.5 mm. (b) Clonogenic activity of the MaSC/basal (Lin-CD29^{hi}CD24⁺hCD4⁺) and luminal (Lin-CD29^{lo}CD24⁺hCD4⁺) populations (1,000 cells) from the mammary glands of 10-week-old MMTV-cre/Mcl-1^{fl/fl} and control mice, grown in Matrigel for 7 days. Scale bar, 0.5 mm. Right: bar graph showing the percentage of colony-forming cells for hCD4⁺ luminal and basal cells. Data are shown as mean \pm s.e.m. for $n=3$ independent experiments ($P=2.54 \times 10^{-11}$; Student's *t*-test). (c) Deletion of Mcl-1 results in a diminished CD61⁺ luminal progenitor subset. Representative

FACS plots ($n=4$) for luminal cells fractionated on the basis of CD61 and CD14 expression. Bar graph (right panel) showing the percentage of each sub-population within the Lin-CD29^{lo}CD24⁺ population isolated from the mammary glands of 10-week-old MMTV-cre/Mcl-1^{fl/fl} or control female mice. Data are shown as mean \pm s.e.m. for $n=4$ mice in each group. $P = 1.59 \times 10^{-5}$, Student's *t*-test for the change in the CD61⁺CD14⁺ subpopulation. (d) Acute deletion of Mcl-1 *in vitro* using cells from Rosa26-creER mice after treatment of cells with 4-OHT *ex vivo* ($n=2$ independent experiments). MaSC/basal or luminal populations purified from mice of the indicated genotypes were cultured in Matrigel and analysed for hCD4 reporter expression at 7 days after induction with 4-OHT for 16 h. (e) Representative images showing the effect of *in vitro* deletion of Mcl-1 on the activity of 1,500 MaSC/basal or luminal progenitor cells in Matrigel ($n=2$). Scale bar, 0.5 mm.

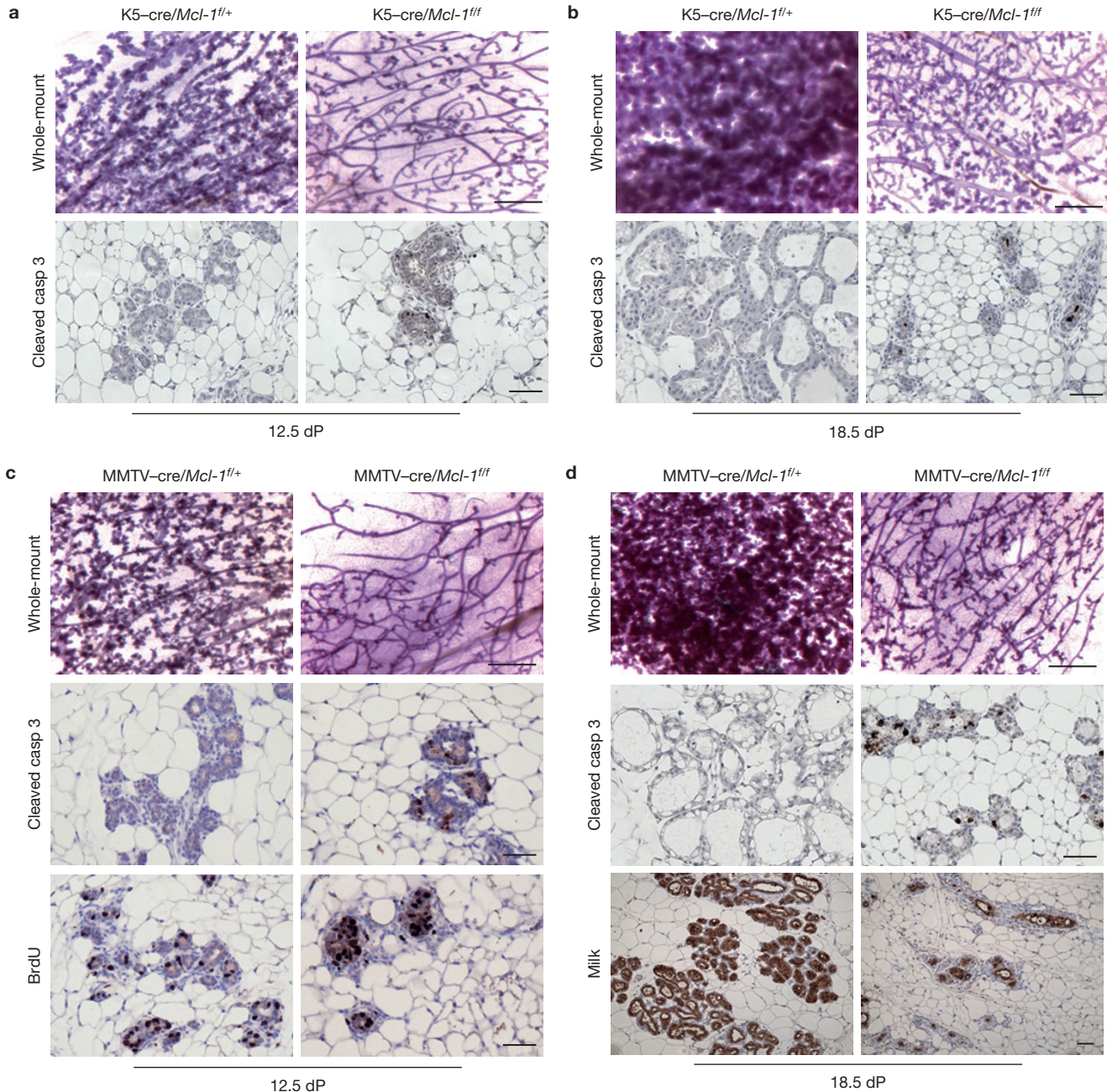


Figure 4 *Mcl-1* deletion impairs alveolar expansion during pregnancy. (a–d) Whole-mount analysis and immunostaining for cleaved caspase-3 of mammary glands at 12.5 or 18.5 days of pregnancy (dP) from *Mcl-1*-deleted or littermate control mice from the K5-cre (a,b) or MMTV-cre (c,d) model.

observed (Fig. 2f), suggesting that *Mcl-1* plays a more important role in the regulation of epithelial cell survival as opposed to expansion. In agreement with fluorescence-activated cell sorting (FACS) analysis of hCD4 reporter expression that demonstrated efficient deletion (Fig. 2g), qRT-PCR analysis confirmed a greater than 90% reduction in *Mcl-1* transcript levels (Fig. 2h). The remaining epithelial cells in MMTV-cre/*Mcl-1*^{f/f} glands lacked *Mcl-1* expression, indicating that selection against these cells had not occurred.

For a,b, representative images for $n=3$ mice of each genotype are shown; for c,d, the images are representative of $n=5$ mice of each genotype. For sections from the MMTV-cre model, immunostaining for BrdU (c) and milk (d) is also shown ($n=3$). Scale bars, 1 mm (whole-mount), 50 μ m (section).

Loss of *Mcl-1* markedly affects stem and progenitor cell activity
 Functional analysis of the different mammary epithelial subsets demonstrated that *Mcl-1* deficiency compromised repopulating potential *in vivo* and clonogenic activity *in vitro*. In transplantation assays, the activity of MaSCs (or their direct descendants) from *Mcl-1*-deficient glands was markedly reduced (Table 1). No outgrowths were generated when cells were transplanted at limiting dilution (100 cells), and only diminutive outgrowths were observed (<10% filling of the fat pad) on implantation of 400 cells (Fig. 3a). Furthermore,

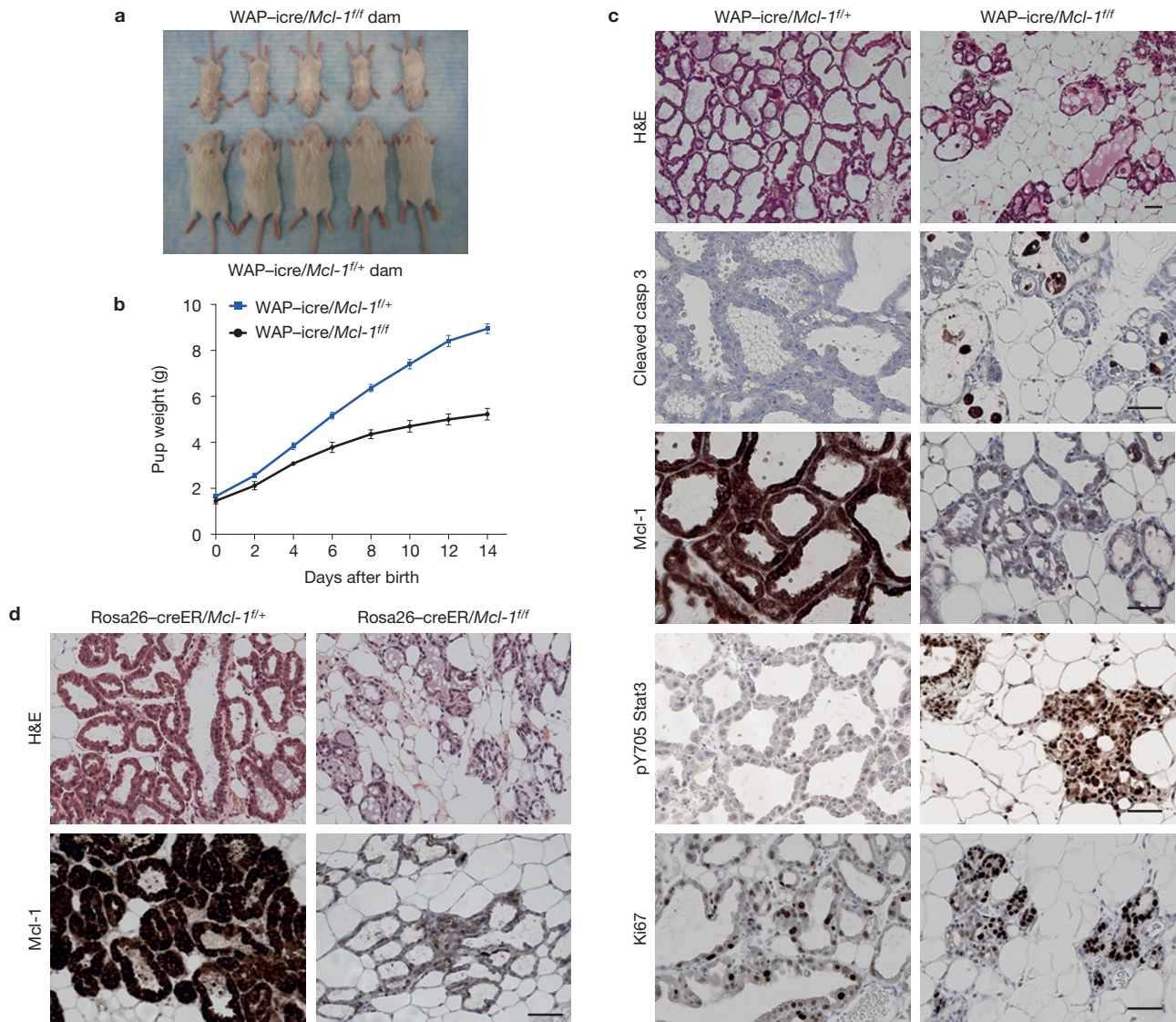


Figure 5 Ablation of *Mcl-1* in early lactation results in precocious involution. **(a,b)** Reduced growth of pups nursed by lactating WAP-cre/Mcl-1^{f/f} dams compared with control littermate females. Pups were weighed every 2 days. Representative photographs of pups are shown in **a**. **(b)** Body weights of pups are shown as the mean \pm s.e.m. (3 dams per arm with 6 pups each; $n=18$), yielding a P value of 1.9×10^{-47} , determined using repeated-measures ANOVA. **(c)** H&E sections or immunohistochemical staining of mammary

glands from WAP-cre/Mcl-1^{f/f} or control dams at 14 days of lactation for cleaved caspase-3, Mcl-1, pY705 Stat3 and Ki-67 ($n=4$ mice per genotype). Scale bars, 50 μ m. **(d)** H&E sections and immunohistochemical staining for Mcl-1 in mammary glands from Rosa26-creER/Mcl-1^{f/f} or control dams at 5 days of lactation (representative of $n=3$ mice per genotype). Deletion of the floxed allele was induced with tamoxifen at 0.5 and 2 days post-partum. Scale bars, 50 μ m.

loss of *Mcl-1* severely impaired the clonogenic capacity of both luminal and basal progenitor cells embedded in Matrigel (Fig. 3b). Interestingly, the CD61⁺ luminal progenitor subset was absent from *Mcl-1*-deficient glands whereas the CD61⁻CD14⁺ alveolar progenitor subset remained, suggesting differential effects of *Mcl-1* loss on distinct progenitor populations within the mammary gland (Fig. 3c). To study the effect of acute deletion of *Mcl-1* on progenitor activity, we isolated epithelial subsets from Rosa26-creER mice for three-dimensional Matrigel cell culture assays. Efficient *Mcl-1* deletion was achieved by treatment with a low concentration of tamoxifen (0.1 μ M), and resulted in markedly reduced progenitor activity in both the luminal and MaSC/basal subsets (Fig. 3d,e).

Mcl-1 deficiency affects alveogenesis and impairs lactation

Analysis of mammary glands during pregnancy from either MMTV-cre/Mcl-1^{f/f} or K5-cre/Mcl-1^{f/f} females indicated an important role for *Mcl-1* in alveolar expansion. The formation of alveolar units was significantly compromised in *Mcl-1*-deficient females at 12.5 and 18.5 days of pregnancy (Fig. 4a-d), as reflected in the presence of small, sparsely distributed alveoli. Apoptosis was augmented following *Mcl-1* deletion, with the appearance of numerous cells positive for cleaved caspase-3 (Fig. 4a-d). The production of milk by the existing alveoli indicated that differentiation was not blocked by *Mcl-1* ablation (Fig. 4d), nor was any change evident in alveolar cell proliferation based on BrdU immunostaining (Fig. 4c). Nevertheless, neither

MMTV-cre/*Mcl-1*^{f/f} nor K5-cre/*Mcl-1*^{f/f} dams were able to nurse their pups, in contrast to heterozygous dams. This resulted in the death of about 70% of pups, lacking milk in their stomachs, within 12 h after parturition and the remainder within 24 h.

To specifically address the role of this pro-survival protein during lactation, we used either WAP-cre or an inducible cre to delete *Mcl-1* after formation of the mature alveolar units. The WAP-cre transgene²³ is active in differentiated secretory cells from early lactation. Examination of WAP-cre/*Mcl-1*^{f/f}, WAP-cre/*Mcl-1*^{f/+} and WAP-cre dams revealed that pups nursed by WAP-cre/*Mcl-1*^{f/f} dams were significantly stunted, with little milk present in their stomachs (Fig. 5a,b). From 6 days of lactation, the glands showed signs of precocious involution, characterized by the loss of alveoli, as well as the presence of increased numbers of apoptotic cells positive for activated caspase-3 and the involution marker pY705 Stat3 (Fig. 5c). No change in proliferating cells was apparent based on Ki-67 staining (Fig. 5c), consistent with findings for MMTV-cre and K5-cre-mediated deletion of *Mcl-1* (Fig. 2f). In the second model, Rosa26-creER/*Mcl-1*^{f/f} dams were treated with tamoxifen immediately after giving birth. By day 5 of lactation, the mammary glands of *Mcl-1*-deficient dams exhibited overt signs of mammary gland involution and no *Mcl-1* was detectable in these cells (Fig. 5d). These mice were analysed before succumbing to other complications such as cardiomyopathy^{15,16}. Both of these lactation-specific models underscore the importance of *Mcl-1* in maintaining the survival of alveolar luminal cells during lactation.

Identification of EGF as a key growth factor upregulated on lactation

We next interrogated potential molecular regulators that could mediate the marked induction of *Mcl-1* expression that occurs on lactogenesis. As noted earlier, *Mcl-1* expression was induced at the protein but not mRNA level, inferring regulation at the post-transcriptional level. RNA-seq analysis was performed on freshly sorted luminal and basal populations from virgin, 18.5-day-pregnant and 2-day-lactating mammary glands. Substantial changes in gene expression were observed in the luminal population between late pregnancy and early lactation, whereas expression changes in MaSC/basal cells were smaller and there was little overlap between differentially expressed genes in the two populations (Fig. 6a). Notably, *Mcl-1* levels were slightly decreased between pregnancy and lactation (Fig. 6b), consistent with qRT-PCR data (Supplementary Fig. 1f). Gene ontology analysis of differentially expressed genes showed enrichment for general metabolic processes, lipid biosynthesis and transport proteins in the luminal compartment, and enrichment for cell contractility genes in the MaSC/basal subset at lactation (Supplementary Table 1), commensurate with the primary function of the gland at this stage²⁴. Gene expression changes in similar functional groups were also observed in microarray studies performed on whole mammary glands²⁵. It is noteworthy that there were no significant changes in the transcript levels of E3 ligases and deubiquitylases known to regulate *Mcl-1* protein turnover^{26,27}. Moreover, no change in the stability of *Mcl-1* protein was evident, based on cycloheximide pulse-chase experiments using sorted cell subpopulations (Supplementary Fig. 3a). Thus, the induction of *Mcl-1* at lactation seems to be independent of transcriptional or protein stabilization mechanisms.

We reasoned that the induction of *Mcl-1* during lactogenesis could be mediated by a cytokine, growth factor or hormonal cue. The lactogenic hormone prolactin was ruled out because treatment of primary mammary epithelial cell cultures with this hormone led to massive induction of milk synthesis but had no impact on *Mcl-1* levels (Supplementary Fig. 3b,c). Notably, EGF was the sixth most upregulated gene in luminal cells and the top-ranked of all differentially expressed cytokines and growth factors (Fig. 6b and Supplementary Fig. 4a). qRT-PCR analysis demonstrated that EGF mRNA was highly expressed in the luminal cells of lactating glands, with a >100-fold increase between late pregnancy and lactation (Fig. 6c). Further interrogation of the expression of the EGF family of ligands and their receptors revealed that expression of the receptor family was relatively constant and that EGF was the only ligand induced in luminal cells at lactogenesis (Supplementary Fig. 4b). *Nrg1* and *Nrg2* were equally high in the MaSC/basal population during late pregnancy and lactation, compatible with the basal cell-specific increase in *Nrg1* previously reported²⁸. In contrast, betacellulin (*Btc*) and amphiregulin (*Areg*) were highly expressed in luminal cells in virgin mammary glands but were downregulated precipitously during lactation. Thus, EGF seems to be exclusively induced at the onset of lactation. It is noteworthy that expression levels of an active form of the EGF receptor (pY1068) were markedly higher during lactation versus late pregnancy (Fig. 6d). To further explore the effect of EGF on *Mcl-1* levels in non-transformed mammary epithelium, a kinetic analysis was performed using HC11 mouse mammary epithelial cells. EGF induced *Mcl-1*, with protein levels peaking at 2–4 h post-treatment, before decreasing to lower levels by 16 h (Fig. 6e). Notably, *Mcl-1* was induced in these cells at the protein but not mRNA level (Fig. 6f), and this occurred concomitantly with phosphorylation of EGFR (Fig. 6e).

EGF mediates induction of *Mcl-1* translation at the onset of lactation

To formally address whether EGF mediates upregulation of *Mcl-1* during lactation, pregnant dams were treated with lapatinib, a dual inhibitor of EGFR (also known as ErbB1) and ErbB2, or vehicle from 17.5 days of pregnancy. Pups nursed by dams that were administered lapatinib had little milk in their stomachs and were stunted in growth (Fig. 6g), and the mammary glands of pregnant dams exposed to lapatinib underwent precocious involution and had markedly decreased levels of *Mcl-1* (Fig. 6h). Cells positive for cleaved caspase-3 were readily detected within the mammary glands of lapatinib-treated mice but were negligible in control glands (Fig. 6h). Given that EGF signalling activates the PI(3)K/mTOR pathway²⁹, we investigated whether exposure to EGF results in increased translation of *Mcl-1*. The mTOR pathway plays a major role in maintaining protein synthesis^{30–32} and *Mcl-1* has been shown to be translationally regulated by mTOR in certain cancer cells^{33,34}. Interestingly, expression of phosphorylated ribosomal protein S6 (pS6; ref. 35), a critical downstream effector of mTOR in the regulation of translation³¹, mirrored that of *Mcl-1* in mammary epithelial cells during lactation and involution (Supplementary Fig. 5a). Moreover, three-dimensional confocal microscopy imaging revealed that high levels of pS6 were restricted to alveolar luminal cells in the lactating mammary gland (Supplementary Fig. 5b), and western blot analysis showed induction of pS6 in EGF-treated HC11 cells (Fig. 6e). In lapatinib-treated mice, expression of pS6 was

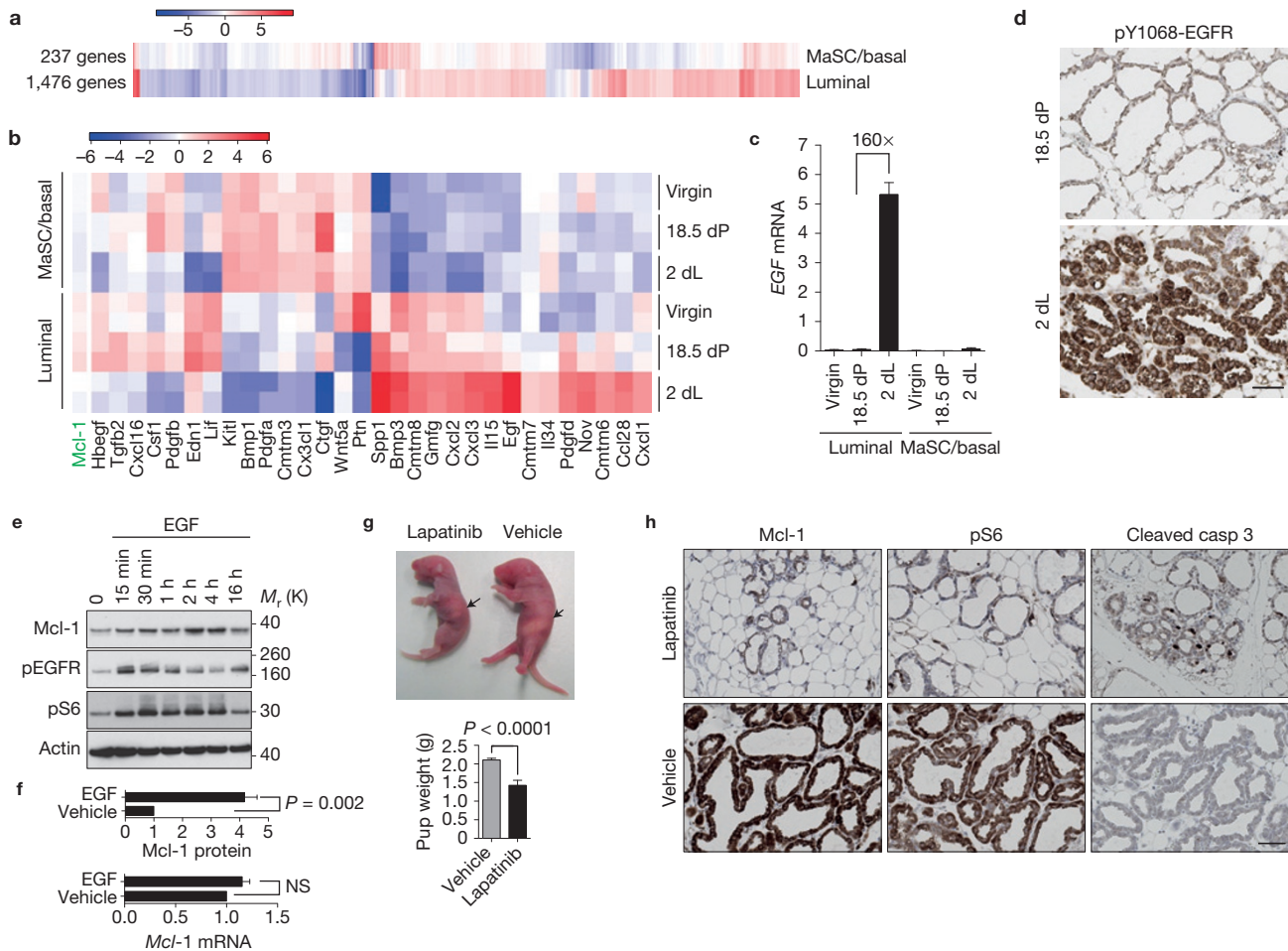


Figure 6 EGF mediates upregulation of Mcl-1 protein at the onset of lactation. **(a)** Heat map showing log₂-fold changes in MaSC/basal and luminal populations. Populations were sorted from mammary glands at 18.5 days of pregnancy and 2 days of lactation. **(b)** Heat map of gene expression for *Mcl-1* and cytokines/growth factors that are differentially expressed between late pregnancy and early lactation for the luminal population. Expression values are on a log₂ scale and are mean-corrected for each gene. Luminal and MaSC/basal cell populations were isolated from virgin, 18.5-day-pregnant (18.5 dP) and 2-day-lactating (2 dL) mammary glands (FVB/N mice). Two independent sorts from the mammary glands of virgin, pregnant or lactating mice were subjected to RNA-seq analysis. **(c)** qRT-PCR analysis for *EGF* in the luminal or MaSC/basal population of mammary glands from virgin, 18.5 dP or 2 dL mice. Data are shown as mean ± s.e.m. for $n=4$ independent mouse samples per genotype. $P=8.23 \times 10^{-5}$ (Student's *t*-test) for the change between 2 dL versus 18.5 dP luminal cells. **(d)** Immunostaining for

pY1068-EGFR in mammary glands at 18.5 dP and 2 dL ($n=3$ for each). Scale bar, 50 μ m. **(e)** Treatment of HC11 mammary epithelial cells with EGF (15 min to 16 h) and western blot analysis to determine the expression of Mcl-1, pEGFR, pS6 and actin. Representative blot of three independent experiments. **(f)** Quantification of Mcl-1 protein levels based on western blot analysis and mRNA levels by qRT-PCR for HC11 cells treated with EGF for 2 h. Data are shown as mean ± s.e.m. for $n=3$ experiments. $P=0.002$; Student's *t*-test. **(g)** Representative photographs of pups nursed by FVB/N dams administered with lapatinib or vehicle. Arrows point to milk in the stomachs of pups. Body weights are shown as mean ± s.e.m. (3 dams per arm nursing 6 pups each; $n=18$). $P=9.14 \times 10^{-8}$ (Student's *t*-test). **(h)** Immunostaining for Mcl-1, pS6 and cleaved caspase-3 in the mammary glands of mothers administrated lapatinib or vehicle at 2 days of lactation (representative of $n=3$ independent experiments). Scale bar, 50 μ m. Uncropped images of blots are shown in Supplementary Fig. 7.

decreased to virtually undetectable levels (Fig. 6h), suggesting that the EGF pathway modulates mTOR signalling during lactation.

To further explore the involvement of the mTOR pathway in alveolar cell function during lactation, mice were treated with the mTORC1 inhibitor RAD001 (everolimus) from late pregnancy. Blockade of mTOR signalling also resulted in failed lactation and a concomitant decrease in pup weight, accompanied by a marked decrease in Mcl-1 and pS6 levels in early lactating glands relative to those from vehicle-treated mice (Fig. 7a,b). Reminiscent of lapatinib-treated mice, numerous cleaved caspase-3-positive cells were now visible in the mammary glands of RAD001-treated

mice (Supplementary Fig. 5c). Compatible with the high levels of pS6, there was a marked global increase in protein translation in lactating mammary glands as measured by sucrose density gradient centrifugation (Fig. 7c). Furthermore, analysis of mRNA distribution within these gradients showed that *Mcl-1*, but not *Bcl-X_L*, mRNA exhibited increased polysome association at both 2 and 4 days of lactation compared with late pregnancy (Fig. 7d; represents averaged data from two biological replicates that are depicted individually in Supplementary Fig. 6). Pertinently, qRT-PCR of *Mcl-1* mRNA extracted from the same samples used for polysome fractionation confirmed that there was no marked increase in *Mcl-1* transcript

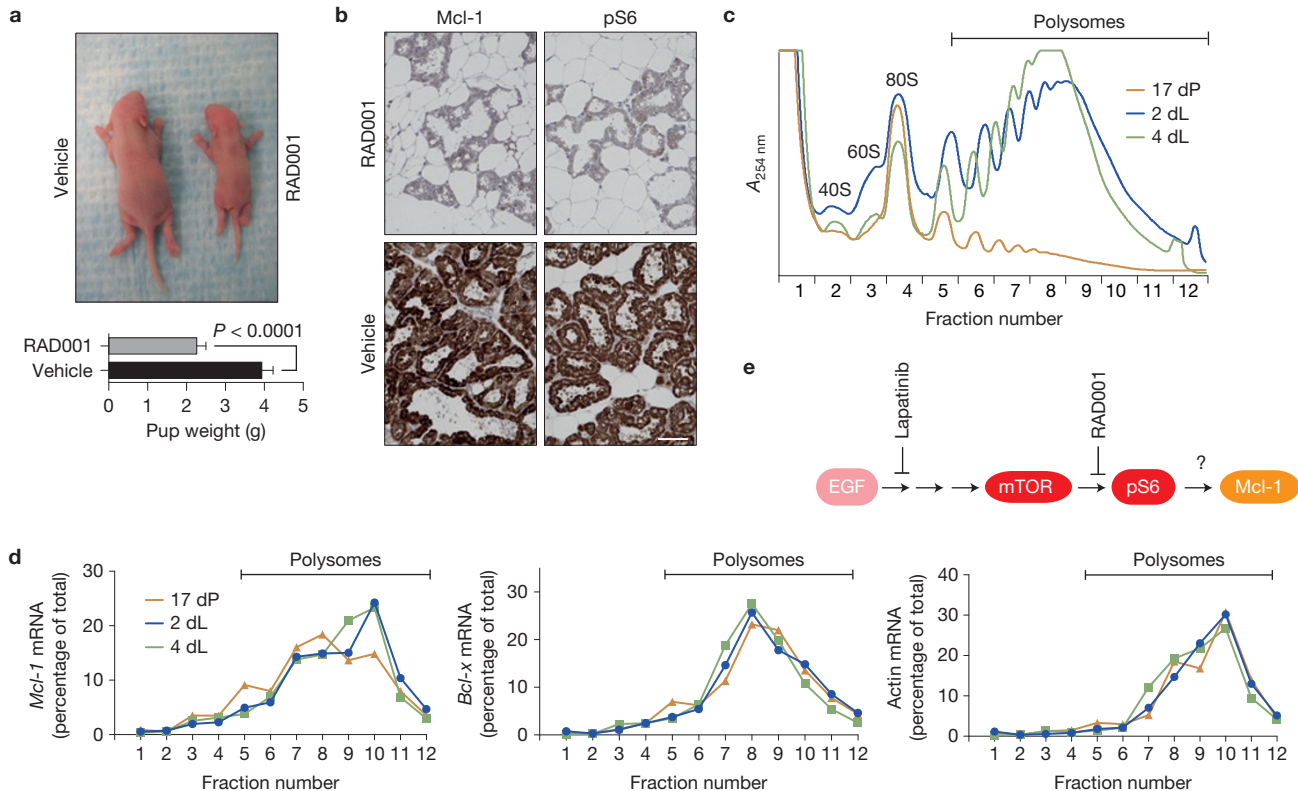


Figure 7 An EGF-mTOR axis mediates upregulation of Mcl-1 protein through increased translation during lactation. **(a)** Representative photographs of pups nursed by FVB/N dams administered RAD001 (everolimus) or vehicle. Pups were weighed at 5 days of lactation. Body weights are shown as mean \pm s.e.m. ($n=3$ dams per group). $P=7.02 \times 10^{-7}$. **(b)** Immunostaining for Mcl-1 and pS6 in the glands of mothers administered RAD001 or vehicle at 5 days of lactation ($n=3$ dams per arm). Scale bar, 50 μm . **(c)** Extracts from mammary glands from 17-day-pregnant (dP), and 2- or 4-day-lactating mice (dL) were fractionated by sucrose density gradient centrifugation. Representative polysome profiles ($A_{254\text{nm}}$: absorbance at 254 nm, dominated

by ribosomal RNA) are shown (independent biological repeats shown in Supplementary Fig. 6a,e). An increase of polysomal complexes relative to 80S monoribosomes is indicative of a global increase in protein translation during lactation. **(d)** Distribution profiles of *Mcl-1*, *Bcl-x* and *Actin* mRNA in polysome fractions isolated from glands at 17 days of pregnancy (dP), and 2 or 4 days of lactation (dL) were measured by qRT-PCR. Data are presented as averages of two independent biological repeat experiments shown individually in Supplementary Fig. 6c,g. **(e)** Schematic model of EGF/mTOR-mediated upregulation of Mcl-1 protein in alveolar cells at the onset of lactation.

levels during lactation (Supplementary Fig. 6d,h), consistent with the RNA-seq data. Collectively, these data suggest that EGF-mediated induction of Mcl-1 at the onset of lactation occurs through mTOR-mediated control of translation.

DISCUSSION

Our data highlight Mcl-1 as a critical regulator of multiple stages of mammary morphogenesis. Mcl-1 regulates the survival of mammary epithelial cells during puberty, pregnancy and lactation. Mcl-1 deficiency at any of these stages resulted in increased numbers of cleaved caspase-3-positive cells, indicative of increased apoptosis. Moreover, Mcl-1 seems to be indispensable for the survival of CD61⁺ luminal progenitor cells, because this population is absent from *Mcl-1*-deficient mammary glands. Mcl-1 is also likely to have an obligate role in MaSCs because the mammary reconstituting frequency of the MaSC population lacking *Mcl-1* was markedly lower than that of control cells and little fat pad filling was observed even when an outgrowth was generated. However, its precise role in these cells awaits the identification of more refined markers, such as Procr (ref. 36), that allow further purification of MaSCs. During lactation, the sole

function of alveolar cells is to produce large amounts of milk protein, lipids and other nutrients, a high-energy requirement that places cells under substantial stress. Neither Bcl-w (ref. 37) nor Bcl-x (ref. 6) plays a role in lactation, and Bcl-2 is unlikely to be essential for this process given that its expression decreases markedly on lactogenesis. Rather, Mcl-1 has emerged as the key pro-survival protein that protects luminal cells from stress-induced cell death during lactation to ensure survival of the offspring.

The profound induction of Mcl-1 at the onset of lactation seems to be largely mediated through EGF (Fig. 7e). Even though deletion of EGF alone may be dispensable for lactogenesis³⁸, mice bearing an EGFR kinase mutation exhibit defective lactation³⁹, suggesting that compensation by other ligands might occur in the case of germline deletion of EGF. Cytokines identified in the gene expression profiling studies, such as IL-15, may also contribute physiologically to the control of Mcl-1 expression. Although our data implicate EGFR/ErbB1, other members of this tyrosine kinase receptor family might be involved in mediating the EGF response through heterodimer formation with ErbB1. For example, ErbB4 deletion in the mammary epithelium has been demonstrated to

lead to aberrant differentiation and lactational failure^{40,41} and could potentially contribute to EGF signalling at the onset of lactation.

EGF seems to play a major role in orchestrating the increased translation of Mcl-1 through the mTOR pathway. Inhibition of EGF signalling with lapatinib or the mTOR pathway through RAD001 markedly curtailed lactation. Pertinently, this was accompanied by marked decreases in Mcl-1 and phosphorylated ribosomal protein S6, as well as increased numbers of apoptotic cells, further supporting a critical role for EGF-mediated Mcl-1 induction in cell survival. Recently, mTOR inhibitor-mediated suppression of Mcl-1 was implicated in priming rhabdomyosarcoma cells for apoptosis⁴². Notably, polysome fractionation studies on whole mammary glands demonstrated that the translation of Mcl-1 but not Bcl-x was specifically augmented during the transition from late pregnancy to lactation. It is noteworthy that the mechanisms regulating Mcl-1 levels are likely to differ substantively between normal and cancerous cells. EGF was recently shown to transcriptionally regulate *Mcl-1* in certain cancer cell lines through the MAPK pathway^{43–45}, whereas we have shown here that transcriptional mechanisms do not contribute to the physiological upregulation of Mcl-1 in mammary epithelial cells during lactation.

In contrast to the prominent expression of Mcl-1 in the lactating mammary gland, the level of Mcl-1 protein declines precipitously at the beginning of involution. Presumably downregulation of this survival factor is required to allow the initiation of apoptosis that has been implicated in the first phase of involution. The exquisite translational regulation of Mcl-1 during mammopoiesis positions it as a crucial regulator of cell survival during lactation and programmed cell death of the alveoli during involution. These findings suggest that Mcl-1 may be the key Bcl-2 family member for the survival of offspring across all mammalian species. □

METHODS

Methods and any associated references are available in the online version of the paper.

Note: Supplementary Information is available in the online version of the paper

ACKNOWLEDGEMENTS

We are grateful to J. Takeda and M. Takaishi for the gift of K5-cre transgenic mice and S. Glaser for provision of mice. We thank D. Huang for advice. We also thank J. L. Clancy, S. K. Archer and G. Duan for assistance with the polysome experiments, B. Helbert for genotyping, and the Animal, FACS, Imaging and Histology facilities at WEHI. This work was supported by the Australian National Health and Medical Research Council (NHMRC) grants no. 1016701, no. 1024852, no. 1086727; NHMRC IRISS; the Victorian State Government through VCA funding of the Victorian Breast Cancer Research Consortium and Operational Infrastructure Support; and the Australian Cancer Research Foundation. N.Y.F. and A.C.R. are supported by a National Breast Cancer Foundation (NBCF)/Cure Cancer Australia Fellowship; A.T.L.L. by an Elizabeth and Vernon Puzey Scholarship from the University of Melbourne; S.A.B. by a NHMRC Postgraduate Scholarship no. 1017256; P.B., G.K.S. and G.J.L. by NHMRC Fellowships no. 1042629, no. 1058892, no. 637307; and J.E.V. by an Australia Fellowship.

AUTHOR CONTRIBUTIONS

N.Y.F. generated and analysed all mouse models, acquired and interpreted main data sets. N.Y.F., G.J.L. and J.E.V. designed experiments. A.C.R. performed confocal microscopy imaging; B.P. qPCR analysis; A.T.L.L. and G.K.S. bioinformatic analysis; R.S. and T.P. polysome fractionation experiments; K.L. assisted with immunohistochemistry; T.B. assisted with western blot analysis; S.A.B. assisted with histological analysis; F.V. performed transplantation assays; P.B. and A.S. provided Mcl-1 mice and discussions. J.E.V. and N.Y.F. wrote the paper.

COMPETING FINANCIAL INTERESTS

The authors declare no competing financial interests.

Published online at www.nature.com/doifinder/10.1038/ncb3117

Reprints and permissions information is available online at www.nature.com/reprints

- Hinck, L. & Silberstein, G. B. Key stages in mammary gland development: the mammary end bud as a motile organ. *Breast Cancer Res.* **7**, 245–251 (2005).
- Watson, C. J. Involution: apoptosis and tissue remodelling that convert the mammary gland from milk factory to a quiescent organ. *Breast Cancer Res.* **8**, 203 (2006).
- Kreuzaler, P. A. *et al.* Stat3 controls lysosomal-mediated cell death *in vivo*. *Nat. Cell Biol.* **13**, 303–309 (2011).
- Czabotar, P. E., Lessene, G., Strasser, A. & Adams, J. M. Control of apoptosis by the BCL-2 protein family: implications for physiology and therapy. *Nat. Rev. Mol. Cell Biol.* **15**, 49–63 (2014).
- Moldoveanu, T., Follis, A. V., Kriwacki, R. W. & Green, D. R. Many players in BCL-2 family affairs. *Trends Biochem. Sci.* **39**, 101–111 (2014).
- Walton, K. D. *et al.* Conditional deletion of the bcl-x gene from mouse mammary epithelium results in accelerated apoptosis during involution but does not compromise cell function during lactation. *Mech. Dev.* **109**, 281–293 (2001).
- Mailleux, A. A. *et al.* BIM regulates apoptosis during mammary ductal morphogenesis, and its absence reveals alternative cell death mechanisms. *Dev. Cell* **12**, 221–234 (2007).
- Opferman, J. T. *et al.* Obligate role of anti-apoptotic MCL-1 in the survival of hematopoietic stem cells. *Science* **307**, 1101–1104 (2005).
- Opferman, J. T. *et al.* Development and maintenance of B and T lymphocytes requires antiapoptotic MCL-1. *Nature* **426**, 671–676 (2003).
- Vikstrom, I. *et al.* Mcl-1 is essential for germlinal center formation and B cell memory. *Science* **330**, 1095–1099 (2010).
- Dzhagalov, I., St John, A. & He, Y. W. The antiapoptotic protein Mcl-1 is essential for the survival of neutrophils but not macrophages. *Blood* **109**, 1620–1626 (2007).
- Steimer, D. A. *et al.* Selective roles for antiapoptotic MCL-1 during granulocyte development and macrophage effector function. *Blood* **113**, 2805–2815 (2009).
- Arbour, N. *et al.* Mcl-1 is a key regulator of apoptosis during CNS development and after DNA damage. *J. Neurosci.* **28**, 6068–6078 (2008).
- Malone, C. D. *et al.* Mcl-1 regulates the survival of adult neural precursor cells. *Mol. Cell. Neurosci.* **49**, 439–447 (2012).
- Thomas, R. L. *et al.* Loss of MCL-1 leads to impaired autophagy and rapid development of heart failure. *Genes Dev.* **27**, 1365–1377 (2013).
- Wang, X. *et al.* Deletion of MCL-1 causes lethal cardiac failure and mitochondrial dysfunction. *Genes Dev.* **27**, 1351–1364 (2013).
- Rios, A. C., Fu, N. Y., Lindeman, G. J. & Visvader, J. E. *In situ* identification of bipotent stem cells in the mammary gland. *Nature* **506**, 322–327 (2014).
- Ertel, F., Nguyen, M., Roulston, A. & Shore, G. C. Programming cancer cells for high expression levels of Mcl1. *EMBO Rep.* **14**, 328–336 (2013).
- Perciavalle, R. M. & Opferman, J. T. Delving deeper: MCL-1's contributions to normal and cancer biology. *Trends Cell Biol.* **23**, 22–29 (2013).
- Thomas, L. W., Lam, C. & Edwards, S. W. Mcl-1; the molecular regulation of protein function. *FEBS Lett.* **584**, 2981–2989 (2010).
- Asselin-Labat, M. L. *et al.* Gata-3 negatively regulates the tumor-initiating capacity of mammary luminal progenitor cells and targets the putative tumor suppressor caspase-14. *Mol. Cell. Biol.* **31**, 4609–4622 (2011).
- Okamoto, T. *et al.* Enhanced stability of Mcl1, a prosurvival Bcl2 relative, blunts stress-induced apoptosis, causes male sterility, and promotes tumorigenesis. *Proc. Natl. Acad. Sci. USA* **111**, 261–266 (2014).
- Wintermantel, T. M., Mayer, A. K., Schutz, G. & Greiner, E. F. Targeting mammary epithelial cells using a bacterial artificial chromosome. *Genesis* **33**, 125–130 (2002).
- Rudolph, M. *et al.* Metabolic regulation in the lactating mammary gland: a lipid synthesising machine. *Physiol. Genomics* **28**, 323–336 (2007).
- Lemay, D. G., Neville, M. C., Rudolph, M. C., Pollard, K. S. & German, J. B. Gene regulatory networks in lactation: identification of global principles using bioinformatics. *BMC Syst. Biol.* **1**, 56 (2007).
- Inuzuka, H. *et al.* SCF(FBW7) regulates cellular apoptosis by targeting MCL1 for ubiquitylation and destruction. *Nature* **471**, 104–109 (2011).
- Schwickart, M. *et al.* Deubiquitinase USP9X stabilizes MCL1 and promotes tumour cell survival. *Nature* **463**, 103–107 (2010).
- Forster, N. *et al.* Basal cell signaling by p63 controls luminal progenitor function and lactation via NRG1. *Dev. Cell* **28**, 147–160 (2014).
- Hynes, N. E. & Lane, H. A. ERBB receptors and cancer: the complexity of targeted inhibitors. *Nat. Rev. Cancer* **5**, 341–354 (2005).
- Ma, X. M. & Blenis, J. Molecular mechanisms of mTOR-mediated translational control. *Nat. Rev. Mol. Cell Biol.* **10**, 307–318 (2009).
- Thoreen, C. C. *et al.* A unifying model for mTORC1-mediated regulation of mRNA translation. *Nature* **485**, 109–113 (2012).
- Wullschleger, S., Loewenthal, R. & Hall, M. N. TOR signaling in growth and metabolism. *Cell* **124**, 471–484 (2006).
- Coloff, J. L. *et al.* Akt-dependent glucose metabolism promotes Mcl-1 synthesis to maintain cell survival and resistance to Bcl-2 inhibition. *Cancer Res.* **71**, 5204–5213 (2011).
- Mills, J. R. *et al.* mTORC1 promotes survival through translational control of Mcl-1. *Proc. Natl. Acad. Sci. USA* **105**, 10853–10858 (2008).

35. Meyuhas, O. Physiological roles of ribosomal protein S6: one of its kind. *Int. Rev. Cell Mol. Biol.* **268**, 1–37 (2008).
36. Wang, D. *et al.* Identification of multipotent mammary stem cells by protein C receptor expression. *Nature* **517**, 81–84 (2015).
37. Print, C. G. *et al.* Apoptosis regulator bcl-w is essential for spermatogenesis but appears otherwise redundant. *Proc. Natl Acad. Sci. USA* **95**, 12424–12431 (1998).
38. Luretteke, N. C. *et al.* Targeted inactivation of the EGF and amphiregulin genes reveals distinct roles for EGF receptor ligands in mouse mammary gland development. *Development* **126**, 2739–2750 (1999).
39. Fowler, K. J. *et al.* A mutation in the epidermal growth factor receptor in waved-2 mice has a profound effect on receptor biochemistry that results in impaired lactation. *Proc. Natl Acad. Sci. USA* **92**, 1465–1469 (1995).
40. Long, W. *et al.* Impaired differentiation and lactational failure of Erbb4-deficient mammary glands identify ERBB4 as an obligate mediator of STAT5. *Development* **130**, 5257–5268 (2003).
41. Muraoka-Cook, R. S., Feng, S. M., Strunk, K. E. & Earp, H. S. III ErbB4/HER4: role in mammary gland development, differentiation and growth inhibition. *J. Mammary Gland Biol. Neoplasia* **13**, 235–246 (2008).
42. Preuss, E., Hugle, M., Reimann, R., Schlecht, M. & Fulda, S. Pan-mammalian target of rapamycin (mTOR) inhibitor AZD8055 primes rhabdomyosarcoma cells for ABT-737-induced apoptosis by down-regulating Mcl-1 protein. *J. Biol. Chem.* **288**, 35287–35296 (2013).
43. Booy, E. P., Henson, E. S. & Gibson, S. B. Epidermal growth factor regulates Mcl-1 expression through the MAPK-Elk-1 signalling pathway contributing to cell survival in breast cancer. *Oncogene* **30**, 2367–2378 (2011).
44. Leu, C. M., Chang, C. & Hu, C. Epidermal growth factor (EGF) suppresses staurosporine-induced apoptosis by inducing mcl-1 via the mitogen-activated protein kinase pathway. *Oncogene* **19**, 1665–1675 (2000).
45. Song, L., Coppola, D., Livingston, S., Cress, D. & Haura, E. B. Mcl-1 regulates survival and sensitivity to diverse apoptotic stimuli in human non-small cell lung cancer cells. *Cancer Biol. Ther.* **4**, 267–276 (2005).

METHODS

Mice. *Mcl-1^{fl/fl}* (ref. 22), MMTV-cre (line A)⁴⁶ and Rosa26-creER^{T2} (TaconicArtemis) have been previously described and were on mixed FVB/C57Bl/6, FVB/N and C57Bl/6 backgrounds, respectively. Keratin 5 (K5)-cre (C57Bl/6 background)⁴⁷ and WAP-icre (FVB/N background)²³ were gifts from J. Takeda (Osaka University, Japan) and G. Schuetz (German Cancer Research Center, Germany), respectively. For timed pregnancies, adult female mice were mated, scored by the presence of vaginal plugs and confirmed by the examination of embryos at the time of mammary gland collection. For lactation experiments, adult female mice were mated with FVB/N stud males and 6 offspring for each litter were maintained. BrdU (0.5 mg per 10 g body weight, Amersham Bioscience) was injected 2 h before mammary gland collection. To inhibit the EGF or mTORC1 pathways, lapatinib (5 mg per mouse, twice per day) or RAD001 (0.5 mg per mouse, daily) were administered respectively by oral gavage, once before birth at 17.5 days of pregnancy and then until collection of glands at 2 days of lactation for lapatinib (GlaxoSmithKline) and 5 days of lactation for RAD001 (Sigma). Rosa26-creER-mediated deletion of the floxed *Mcl-1* allele was carried out by administering tamoxifen (3 mg) to lactating mothers at 0.5 and 2 days of lactation by oral gavage. All experiments were conducted with the approval of and according to the guidelines of the Walter and Eliza Hall Institute of Medical Research Animal Ethics Committee.

A minimum of three female mice were analysed for each genotype and for each developmental time point. Mice were subjected to the indicated analysis, and the numbers of mice and independent biological experiments are stated in the figure legends. No statistical method was used to predetermine sample size and the experiments were not randomized. The investigators were not blinded in the analysis of the knockout mouse phenotype, as the correct genotype needed to be studied. In addition, the profound phenotype of knockout animals made blinding impossible. For the drug treatments of mice, all injections were carried out in a blinded fashion by the mouse research technician. The investigator then removed the mammary glands according to the marking on the boxes that were made by the research technician.

Mammary cell preparation, FACS analysis and cell sorting. Mammary glands were collected from female mice, and single-cell suspensions were prepared as previously described⁴⁸. The following FACS antibodies were used: biotin-anti-mouse CD14 (rat, clone Sa2-8) from eBioscience; APC/cy7 anti-mouse/rat CD29 (rat, clone HMβ1-1), Pacific blue anti-mouse CD24 (rat, clone M1/69) and PE-anti-mouse/rat CD61 (rat, clone HM63-1) from BioLegend; PE-anti human CD4 (mouse, clone L120) antibodies, APC anti-mouse CD31 (rat, clone MEC13.3), APC anti-mouse CD45 (rat, clone 30-F11), APC anti-mouse Ter119 (rat, clone Ter-119) antibodies from BD PharMingen. To exclude dead cells, cells were re-suspended in approximately 0.2 µg ml⁻¹ 7-AAD (Sigma) before analysis. Cell sorting was performed on the FACS Aria (Becton Dickinson). FACS data were analysed using FlowJo software (Tree Star). The Lin⁻ population was defined by Ter119⁻CD31⁻CD45⁻.

Histology and whole-mounting of mammary glands. Mammary glands were fixed in 4% paraformaldehyde, embedded in paraffin, sectioned and stained with haematoxylin and eosin (H&E). For whole-mount analysis, mammary glands were fixed in Carnoy's solution containing 60% ethanol, 30% chloroform and 10% glacial acetic acid at room temperature for at least 16 h before staining with carmine alum.

Transplantation and *in vitro* colony-forming or differentiation assays. Freshly sorted CD29^{hi}CD24⁺hCD4⁺ cells from 10-week-old mice were implanted into the cleared inguinal glands of 3-week-old syngeneic recipient mice, as described previously⁴⁸. FACS-sorted populations were counted and serially diluted in buffer (40% FCS, 10% trypan blue, 25% growth-factor-reduced Matrigel (BD PharMingen) in PBS) before transplantation. Limiting dilution analysis was performed as described previously⁴⁸.

For colony-forming assays, sorted mammary luminal or basal cells were embedded in Matrigel (BD PharMingen) as described previously⁴⁸ and cultured for 7–8 days. For deletion of *Mcl-1* *in vitro*, sorted cells from the mammary glands of Rosa26-creER/*Mcl-1* females were cultured in Matrigel for 24 h before treatment with 0.1 µM 4-hydroxy-tamoxifen (4-OHT) for 16 h, followed by culture in normal medium for another 7–8 days. For induction of differentiation and milk production, primary mammary epithelial cells (Lin⁻CD24⁺) were cultured in growth-factor-reduced Matrigel for 7 days, and starved in serum-free medium for 36 h before induction with 500 µg ml⁻¹ hydrocortisone plus 5 µg ml⁻¹ prolactin in medium containing 2% horse serum for 3 days.

EGF treatment of HC11 cells. HC11 mouse mammary epithelial cells were maintained in RPMI1640 medium containing 2 mM L-glutamine, supplemented with 10% fetal calf serum and 4 µg ml⁻¹ insulin, 10 ng ml⁻¹ epidermal growth factor (EGF) and 10 mM HEPES, at 37 °C in 5% CO₂. For induction experiments, confluent cells were incubated for 6 h in RPMI 1640 medium containing 2% horse serum,

4 µg ml⁻¹ insulin, 500 µg ml⁻¹ hydrocortisone and 5 µg ml⁻¹ prolactin, and then treated with 100 ng ml⁻¹ EGF for the indicated time periods.

Cycloheximide pulse-chase experiments. Sorted mammary luminal cells (Lin⁻CD29^{lo}CD24⁺) from 18.5-day-pregnant or 2-day-lactating mouse mammary glands were plated in 24-well ultralow-adherence plates (Corning) in mammosphere medium (DMEM/F12 + Glutamax, 1% penicillin/streptomycin, 10 ng ml⁻¹ bFGF, 5 µg ml⁻¹ insulin, 500 µg ml⁻¹ hydrocortisone, B27 supplement) and cultured for 15 min before cells were treated with 100 µg ml⁻¹ cycloheximide for different time periods, as described previously⁴⁹. Cells were collected and analysed by western blotting for Mcl-1 protein levels.

Western blot analysis and immunohistochemistry. FACS-sorted cells were directly lysed in the RIPA buffer containing 1× complete mini protease inhibitor cocktail (Roche) and 1× Roche PhosSTOP phosphatase inhibitor cocktail (Roche). Whole mammary gland lysates were prepared by grinding tissue in liquid nitrogen and solubilizing in RIPA buffer. The following primary antibodies were used for western blot analysis: anti-Mcl-1 (rabbit, clone D35A5, 1:500 dilution), anti-Bim (rabbit, clone C34C5, 1:500 dilution), anti-Bcl-xL (rabbit, clone 54H6, 1:500 dilution), anti-Stat3 (rabbit, 1:500 dilution), anti-phospho-Stat3 (Tyr 705; rabbit, clone D3A7, 1:500 dilution) and anti-phospho-EGFR (Tyr 1068; rabbit, clone D7A5, 1:500 dilution) from Cell Signaling; anti-actin (mouse, clone AC-15, 1:5,000 dilution) and anti-tubulin (mouse, clone B-5-1-2, 1:5,000 dilution) from Sigma; anti-Bcl-2 (mouse, clone C-2, 1:500 dilution) from Santa Cruz; rat anti-Bcl-w (1:100 dilution) and A1 (1:50 dilution) antibodies were provided by A.S., L. O'Reilly and M. Herold (The Walter and Eliza Hall Institute of Medical Research, Australia).

Immunohistochemical detection of BrdU-labelled cells was performed as per the manufacturer's protocol using rat anti-BrdU antibody (Accurate Chemical and Scientific and Corporation, OBT0030G; 1:100 dilution). For other immunohistochemical staining, the following antibodies were used: anti-Mcl-1 (rabbit, clone D35A5, 1:100-400 dilution), anti-pS6 (rabbit, clone D68F8, 1:400 dilution), anti-phospho-Stat3 (Tyr 705; rabbit, clone D3A7, 1:100 dilution), and anti-phospho-EGFR (Tyr 1068; rabbit, clone D7A5, 1:100 dilution) and anti-cleaved (that is, activated) caspase-3 (rabbit, clone D3E9, 1:100 dilution) from Cell Signaling. An isotype-matched control IgG was used as the negative control. The streptavidin-biotin-peroxidase detection system was used with 3,3'-diaminobenzidine as substrate (DAKO).

For immunohistochemistry and western blot analysis, representative images are shown; the number of independent samples and biological experiments performed is indicated in the figure legends.

Whole-mount mammary gland preparation for confocal microscopy imaging. Tissues were fixed in 4% paraformaldehyde and incubated overnight at 4 °C with primary antibody. The following day, tissues were incubated overnight with secondary antibody and phalloidin (1:50; Invitrogen). Tissues were subsequently incubated in 80% glycerol before dissection for three-dimensional imaging, as previously described¹⁷. Primary antibodies: Mcl-1 (rabbit, clone D35A5, Invitrogen; 1:200 dilution), pS6 (rabbit, clone D68F8, Invitrogen; 1:200 dilution) and E-cadherin (rat, clone ECCD-2, Invitrogen; 1:200 dilution). Secondary antibody: anti-rabbit Alexa Fluor 488 (Invitrogen). F-actin was stained with Alexa Fluor 647 phalloidin (Invitrogen; 1:50 dilution).

qRT-PCR analysis. Total RNA was prepared from FACS-sorted mammary epithelial subpopulations with the RNeasy Micro kit (Qiagen). Complementary DNA synthesis and qRT-PCR analysis were performed and normalized against 18S ribosomal RNA, as described previously⁵⁰. See below for qRT-PCR analysis of polysome gradient fractions.

RNA-seq analysis. Total RNA was extracted from sorted luminal or basal populations from the mammary glands of virgin, 18.5-day-pregnant and 2-day-lactating FVB/N female mice (two independent samples per stage). Total RNA (100 ng) was used to generate libraries for whole-transcriptome analysis following Illumina's TruSeq RNA v2 sample preparation protocol. Libraries were sequenced on an Illumina HiSeq 2000 at the Australian Genome Research Facility (AGRF), Melbourne. At least 20 million 100 bp single-end reads were obtained for each sample. Reads were aligned to the mouse genome mm10 using Rsubread version 13.25 (ref. 51). The number of reads overlapping each Entrez gene was counted using RefSeq gene annotation and featureCounts⁵¹. Filtering and normalization used the edgeR package⁵². Genes were filtered as unexpressed if their average count per million (CPM) computed by the aveLogCPM function was less than one. Compositional differences between libraries were normalized using the trimmed mean of M-values (TMM) method⁵³. Differential expression was analysed using the Limma package⁵⁴. Counts were transformed to log₂-CPM values with associated precision weights using voom⁵⁵. Differential expression was assessed using the TREAT method⁵⁶, whereby differential expression is evaluated relative to a biologically meaningful

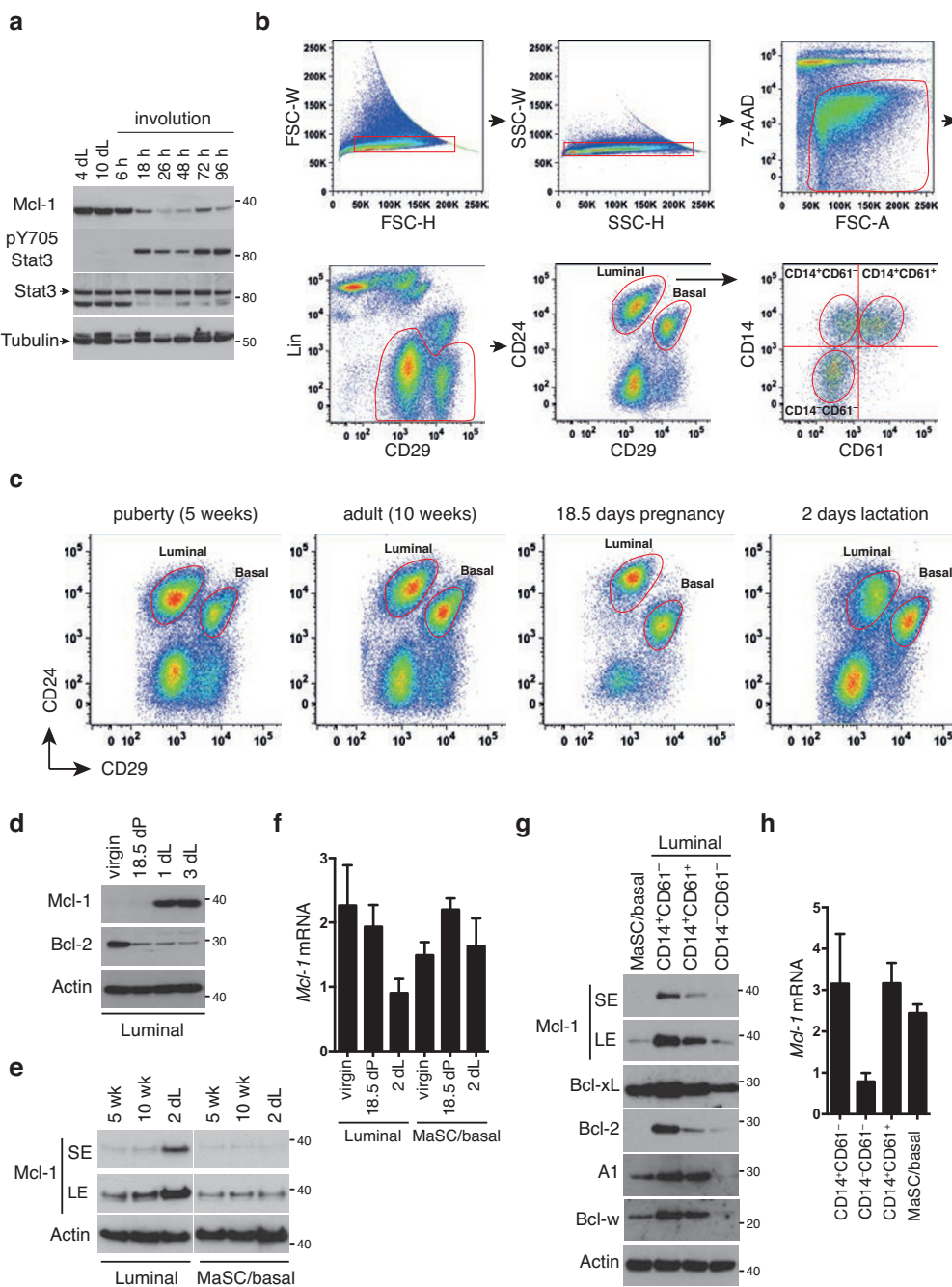
fold-change threshold. Genes were considered to be differentially expressed if they achieved a false discovery rate of 1% in exceeding a fold-change of 1.5. Gene ontology analysis used the goseq package⁵⁷, which corrects the analysis for gene length bias. Log-CPM values shown in heat maps were computed using the edgeR package with a prior.count of 3 to reduce variability at low counts.

Polysome profile analysis. Extracts were prepared from murine mammary glands and polysome fractionation was carried out essentially as described previously^{58,59} with some modifications. Glands from virgin, late-pregnant (d16.5–17.0) or lactating (2 dL and 4 dL) mice ($n = 2$ for each time-point) were flash-frozen in liquid nitrogen and ground to a homogeneous powder. Lysis buffer (1 ml of buffer containing 20 mM HEPES (pH 7.6), 125 mM KCl, 5 mM MgCl₂, 10 mM dithiothreitol, 1% DOC, 1% NP-40, 0.1 mg ml⁻¹ cycloheximide, 1× cComplete EDTA-free protease inhibitor cocktail (Roche), 1 mM phenylmethylsulphonyl fluoride, 400 U ml⁻¹ RNaseOUT (Life Technologies)) was then added with vortexing. Cell debris was removed from thawed lysates by centrifugation (16,000 g, 10 min, 4°C). Cleared lysates (approximately 25 A_{260nm} units) were loaded onto linear sucrose density gradients (17.5–50% (w/v) in lysis buffer without detergents, cComplete inhibitors and RNaseOUT) and centrifuged for 2 h 15 min at 35,000 g at 4°C in a SW41 Ti rotor (Beckman Coulter). Gradients were displaced from the bottom up by a chase solution (60% sucrose) at a rate of 0.75 ml min⁻¹, passed through an ultraviolet detector to obtain a continuous A_{254nm} profile, and collected into 12 fractions using a Brandel BR-188 system at 4°C. Each gradient fraction was spiked with 20 µg of glycogen and 20 pg of an *in vitro*-transcribed *Renilla* luciferase RNA (3xB RL; ref. 60) and precipitated with 3 volumes of ethanol overnight at –80°C. After centrifugation, RNA was extracted from the pellets with Trizol (Life Technologies) as per the manufacturer's instructions with an additional sodium acetate/ethanol precipitation. The mRNA level of *Mcl-1*, *Bcl-x* and *actin* in each gradient fraction was analysed by qRT-PCR performed on a QuantStudioTM 12K Flex system (Life Technologies) using a Fast SYBR Green Master Mix (Life Technologies). qPCR data from each fraction were first normalized to the 3xB RL spike-in and then expressed as a percentage of total signal across all 12 fractions per gradient. Primer sequences: (5'-3') *Mcl-1* F: 5'-TG TAAGGACGAAACGGGACT-3', *Mcl-1* R: 5'-AAAGCCAGCAGCACATTCT-3', *BCL-x* F: 5'-GACAAGGAGATGCAGGTATTGG-3', *BCL-x* R: 5'-TCCCGTAGAG ATCCACAAAAGT-3', *RL* F: 5'-GGCGAGAAAATGGTGCTTGAG-3', *RL* R: 5'-TC CTTGAATGGCTCCAGGTAGG-3'. *Actb* F: 5'-CGGTTCCGATGCCCTGAGG CTCTT-3', *Actb* R: 5'-CGTCACACTTCATGATGGAATTGA-3'.

Statistical analysis. Data are shown as mean ± standard error of the mean (s.e.m.). The Student's *t*-test was used where applicable, with $P < 0.05$ considered significant.

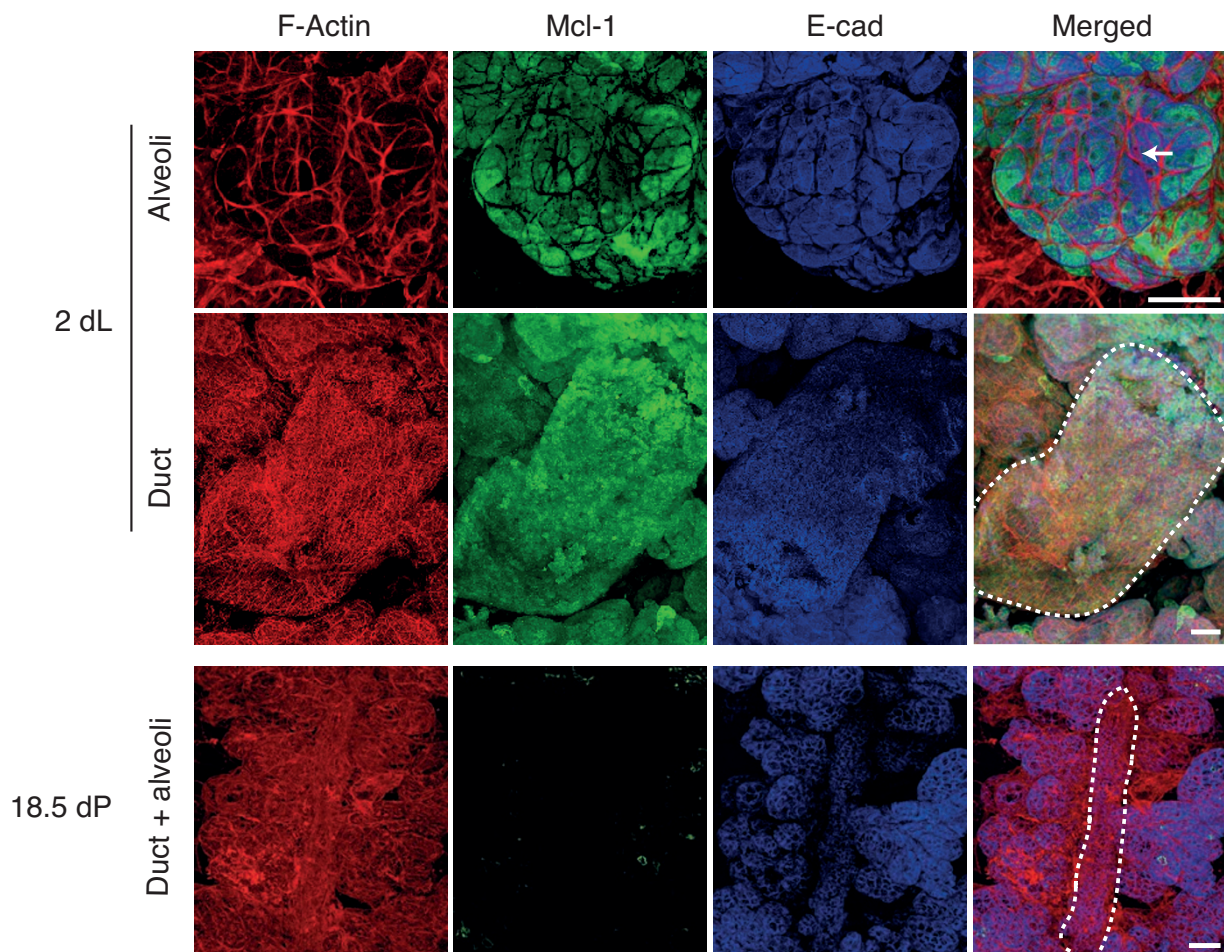
Accession number. RNA-seq data are deposited in the Gene Expression Omnibus with accession no. [GSE60450](#).

46. Wagner, K. U. *et al.* Cre-mediated gene deletion in the mammary gland. *Nucleic Acids Res.* **25**, 4323–4330 (1997).
47. Tarutani, M. *et al.* Tissue-specific knockout of the mouse Pig-a gene reveals important roles for GPI-anchored proteins in skin development. *Proc. Natl. Acad. Sci. USA* **94**, 7400–7405 (1997).
48. Shackleton, M. *et al.* Generation of a functional mammary gland from a single stem cell. *Nature* **439**, 84–88 (2006).
49. Fu, N. Y., Sukumaran, S. K., Kerk, S. Y. & Yu, V. C. Baxbeta: a constitutively active human Bax isoform that is under tight regulatory control by the proteasomal degradation mechanism. *Mol. Cell* **33**, 15–29 (2009).
50. Pal, B. *et al.* Global changes in the mammary epigenome are induced by hormonal cues and coordinated by Ezh2. *Cell Rep.* **3**, 411–426 (2013).
51. Liao, Y., Smyth, G. K. & Shi, W. featureCounts: an efficient general purpose program for assigning sequence reads to genomic features. *Bioinformatics* **30**, 923–930 (2014).
52. Robinson, M. D., McCarthy, D. J. & Smyth, G. K. edgeR: a Bioconductor package for differential expression analysis of digital gene expression data. *Bioinformatics* **26**, 139–140 (2010).
53. Robinson, M. D. & Oshlack, A. A scaling normalization method for differential expression analysis of RNA-seq data. *Genome Biol.* **11**, R25 (2010).
54. Smyth, G. K. Linear models and empirical Bayes methods for assessing differential expression in microarray experiments. *Stat. Appl. Genet. Mol. Biol.* **3**, 1–25 (2004).
55. Law, C. W., Chen, Y., Shi, W. & Smyth, G. K. Voom: precision weights unlock linear model analysis tools for RNA-seq read counts. *Genome Biol.* **15**, R29 (2014).
56. McCarthy, D. J. & Smyth, G. K. Testing significance relative to a fold-change threshold is a TREAT. *Bioinformatics* **25**, 765–771 (2009).
57. Young, M. D., Wakefield, M. J., Smyth, G. K. & Oshlack, A. Gene ontology analysis for RNA-seq: accounting for selection bias. *Genome Biol.* **11**, R14 (2010).
58. Clancy, J. L. *et al.* Methods to analyze microRNA-mediated control of mRNA translation. *Methods Enzymol.* **431**, 83–111 (2007).
59. Stoezlé, T., Schwab, P., Trumpp, A. & Hynes, N. E. c-Myc affects mRNA translation, cell proliferation and progenitor cell function in the mammary gland. *BMC Biol.* **7**, 63 (2009).
60. Pillai, R. S. *et al.* Inhibition of translational initiation by Let-7 microRNA in human cells. *Science* **309**, 1573–1576 (2005).

**Supplementary Figure 1** Expression of Mcl-1 in the mammary gland.

(a) Western blots showing the rapid decrease of Mcl-1 at the onset of involution. pY705 Stat3 represents a marker for involution ($n=2$ independent experiments). (b) General strategy for flow cytometric analysis and sorting of mammary epithelial cells. Representative FACS plots ($n=10$) showing the MaSC/basal ($\text{Lin}^- \text{CD29}^{\text{hi}} \text{CD24}^+$) and luminal ($\text{Lin}^- \text{CD29}^{\text{lo}} \text{CD24}^+$) subsets. The luminal population was further subdivided into three distinct subpopulations based on CD14 and CD61 expression: $\text{CD14}^+\text{CD61}^-$, $\text{CD14}^+\text{CD61}^+$ and $\text{CD14}^-\text{CD61}^-$. (c) Representative FACS plots ($n=8$) showing the MaSC/basal ($\text{Lin}^- \text{CD29}^{\text{hi}} \text{CD24}^+$) and luminal ($\text{Lin}^- \text{CD29}^{\text{lo}} \text{CD24}^+$) subsets isolated from the mammary glands of 5 week-old (puberty), 10 week-old adult (virgin), 18.5 day pregnant (18.5 dP) and 2 day lactating (2 dL) mice. (d) Western blots showing the decrease in Bcl-2

levels in luminal cells that occurs during pregnancy and lactation relative to virgin glands ($n=1$). (e) Representative Western blots showing Mcl-1 levels in luminal and MaSC/basal cells in puberty versus adult and 2 day lactating mammary glands, with short (SE) and long exposures (LE) indicated. (f) Quantitative RT-PCR analysis of *Mcl-1* mRNA in the luminal or MaSC/basal population of mammary glands from virgin, 18.5 day pregnant (18.5 dP) or 2 day lactating (2 dL) mice. Mean \pm SEM for $n=3$ independent samples. (g) Western blot analysis of Bcl-2 family protein expression in the four distinct mammary epithelial cell subsets of virgin mammary glands. Approximately 250,000 cells were used for each sample ($n=1$). (h) Quantitative RT-PCR analysis of *Mcl-1* expression in luminal (progenitor and mature) or MaSC/basal populations isolated from virgin mammary glands. Mean \pm SEM, $n=3$ independent samples.

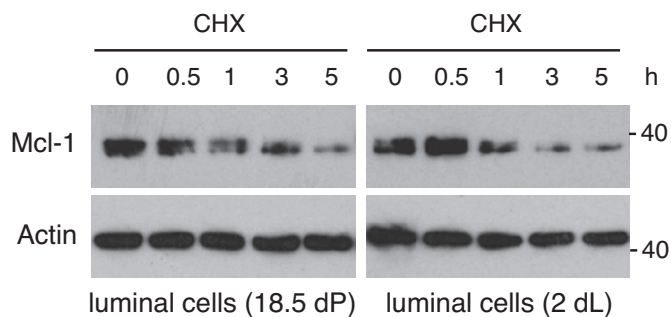


Supplementary Figure 2 Mcl-1 protein is induced in ductal and alveolar luminal cells at the switch to lactation. Whole-mount 3D confocal images of mammary glands at 2 days of lactation (2 dL) or 18.5 days of pregnancy, showing ducts and/or alveoli. The tissues were stained for F-actin (red),

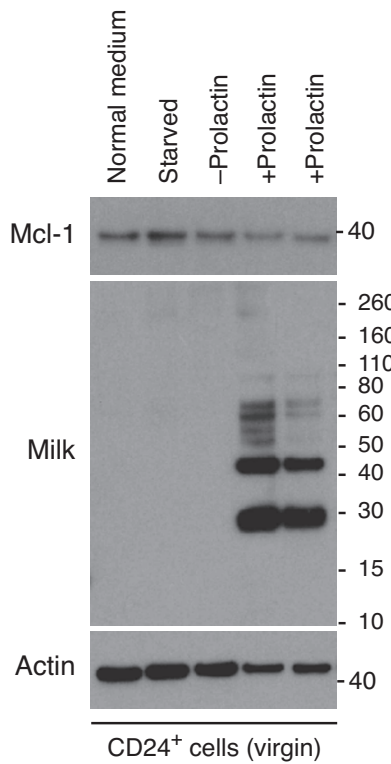
Mcl-1 (green) and E-cadherin (blue) expression. An outline of the ducts is depicted in the merged images. The white arrow depicts the mesh of elongated myoepithelial cells that surround each alveolus. Representative of 3 experiments. Scale bars, 50 μ m.

SUPPLEMENTARY INFORMATION

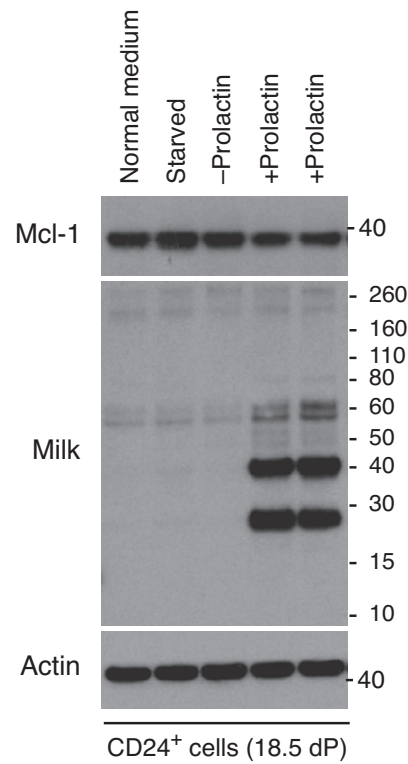
a



b

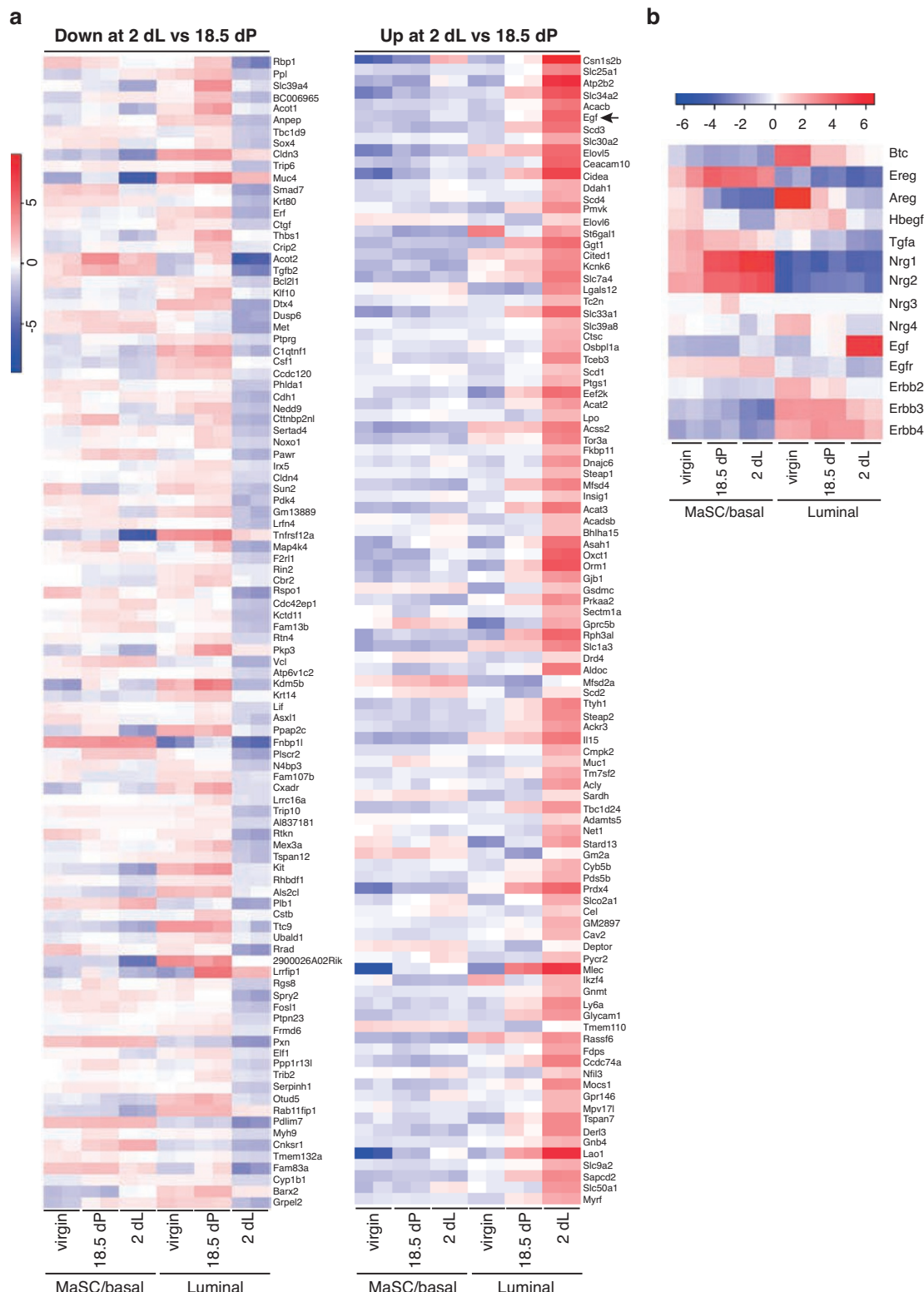


c



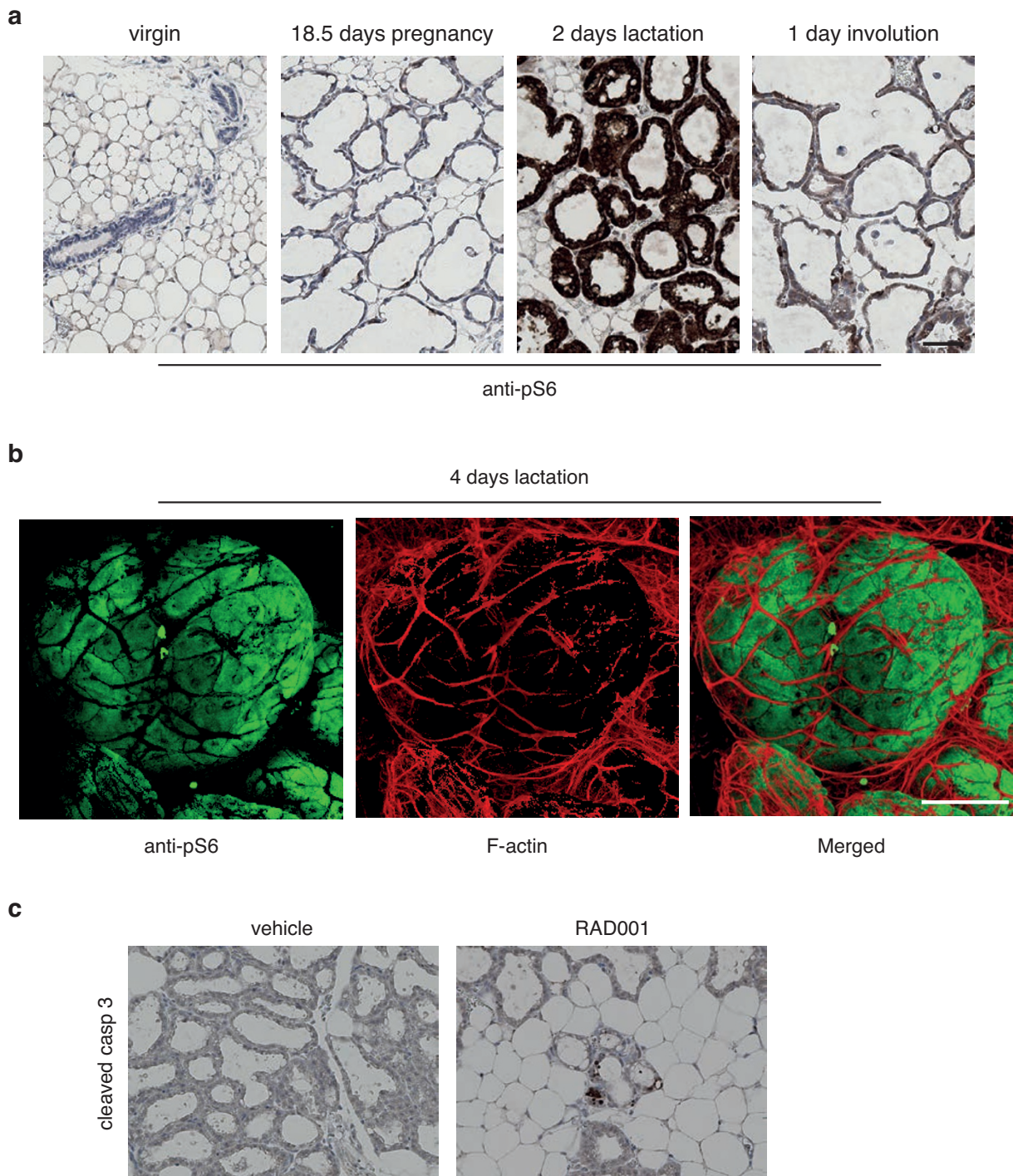
Supplementary Figure 3 No apparent change in the stability of Mcl-1 based on cycloheximide pulse-chase experiments and no induction of Mcl-1 by prolactin. **(a)** Luminal cells ($\text{Lin}^-\text{CD29}^{\text{lo}} \text{CD24}^+$) were sorted from the mammary glands of 18.5 day pregnant or 2 day lactating mice, plated in ultra-low adherence plates and incubated with cycloheximide (CHX) for the indicated times. Lysates were subjected to western blot

analysis for Mcl-1 and Actin protein levels (n=2 experiments). **(b, c)** Mammary epithelial cells ($\text{Lin}^-\text{CD24}^+$) were sorted from virgin (b) or 18.5 day pregnant (c) mammary glands, starved of serum and EGF for 36 h and exposed to the lactogenic hormone prolactin for 3 days. Western blot analysis was performed to determine Mcl-1, milk and actin protein expression (n=1).



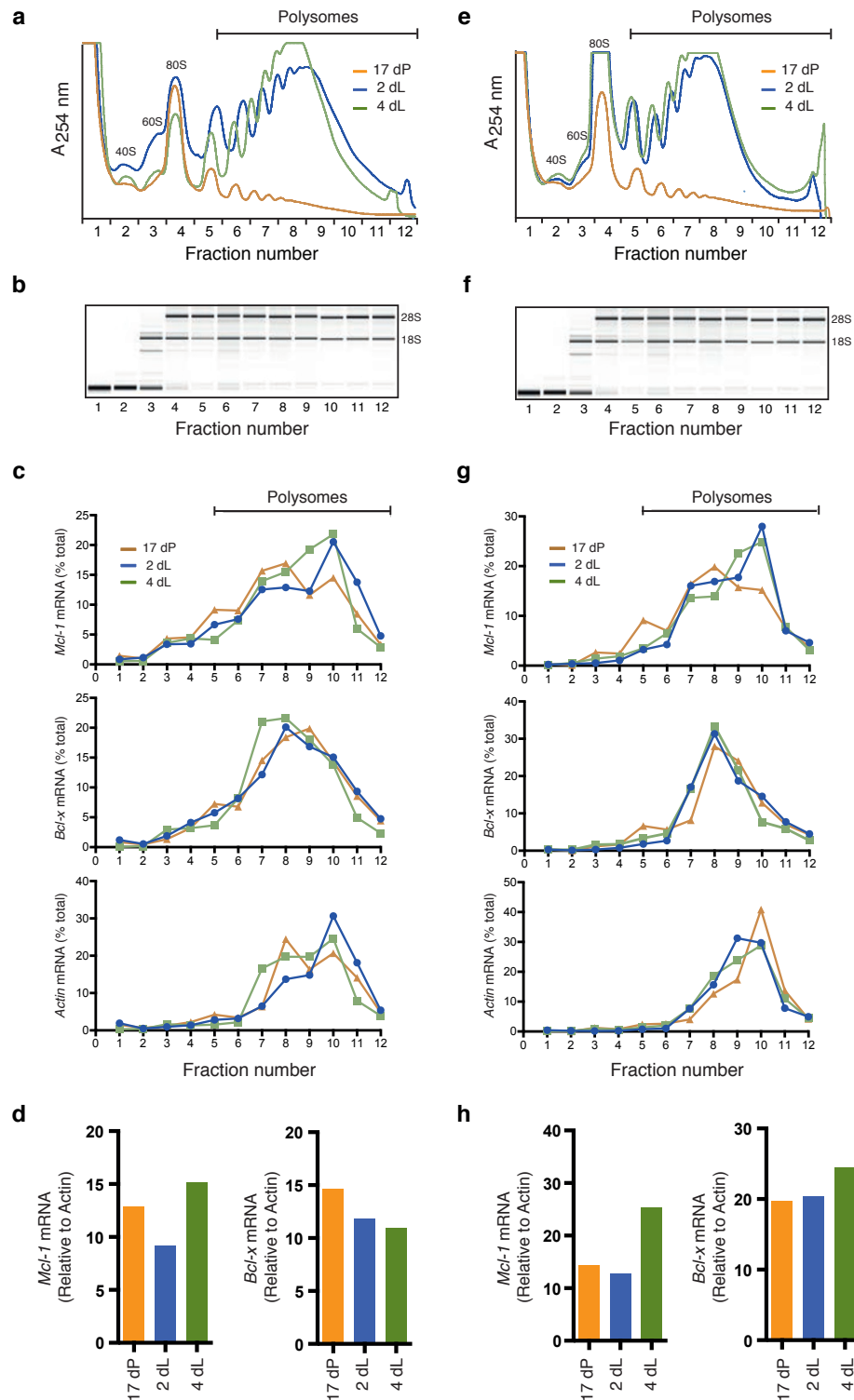
(18.5 dP) and 2 day lactating (2 dL) mammary glands (FVB/N). (c) Heatmap of gene expression for members of the EGF receptor/ligand family that are differentially expressed between late pregnancy and early lactation for the luminal population. 18.5 dP or 2 dL mice. dP, days pregnancy; dL, days lactation.

SUPPLEMENTARY INFORMATION



Supplementary Figure 5 Increased phospho-S6 expression in alveolar luminal cells at the onset of lactation. **(a)** Immunostaining of phospho-S6 protein in the mammary glands of FVB/N mice (n=2 mice per stage) through development. Scale bar: 50 μ m. **(b)** 3D whole-mount confocal analysis of pS6 in the mammary glands of FVB/N mice (n=3) at 4 days of lactation.

Tissues were incubated with Phalloidin to observe the entire tissue at the cellular level. Scale bar: 50 μ m. **(c)** Immunostaining for cleaved caspase 3 in the mammary glands isolated from mothers administrated RAD001 or vehicle at 2 days of lactation (n=3 dams). Scale bar: 50 μ m. Representative images (a-c) are shown for n=3 experiments.



Supplementary Figure 6 Polysome profiles and RNA expression data from mammary tissue from 17 days pregnant (dP), and 2 or 4 days lactating mice (dL). Data for two independent biological repeat experiments are shown: Experiment 1 (**a-d**) and Experiment 2 (**e-h**). (**a, e**) Polysome fractionation profiles (A254: absorbance at 254 nm, dominated by ribosomal RNA) from mammary gland tissue; (**b, f**) Representative graphs from one gradient per

experiment showing RNA integrity across gradient fractions as determined on the Agilent Bioanalyzer; (**c, g**) Distribution of *Mcl-1*, *Bcl-x* and *Actin* mRNA amongst gradient fractions isolated from mammary glands at 17 dP, 2 dL and 4 dL; (**d, h**) Quantitative RT-PCR analysis of *Mcl-1*, *Bcl-x* and *Actin* mRNA steady-state levels in the unfractionated cell lysates used for polysome fractionation (mean of 3 technical replicates).

SUPPLEMENTARY INFORMATION

Figure 1b

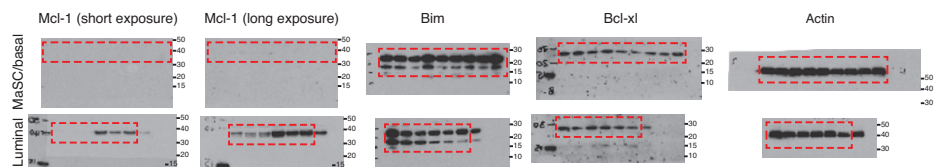
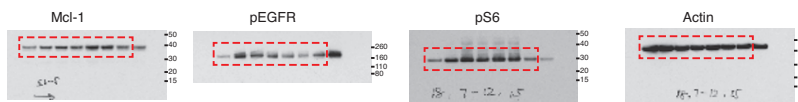
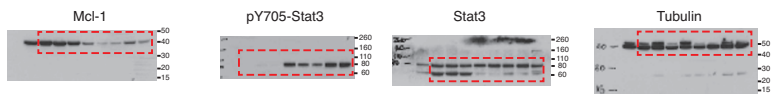


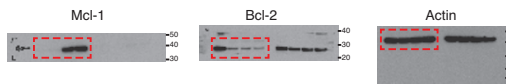
Figure 6d



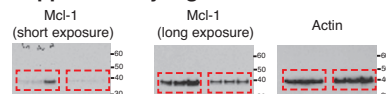
Supplementary Figure 1a



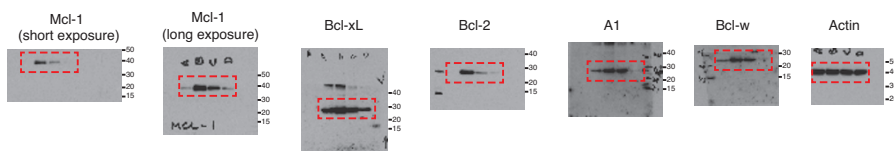
Supplementary Figure 1d



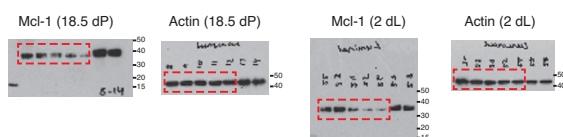
Supplementary Figure 1e



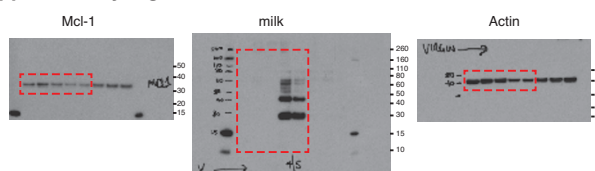
Supplementary Figure 1g



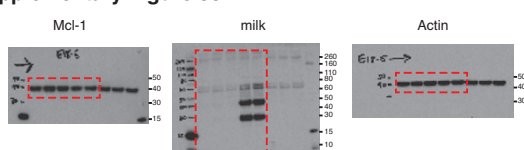
Supplementary Figure 3a



Supplementary Figure 3b



Supplementary Figure 3c



Supplementary Figure 7 Uncropped scans of western blots.

Supplementary Table Legend

Supplementary Table 1 Gene ontology analysis of differentially expressed genes in the luminal and MaSC/basal populations from pregnant versus lactating mammary glands. Gene ontology terms representing biological processes that are over-represented amongst differentially expressed genes in the luminal and MaSC/basal populations.